NBER WORKING PAPER SERIES

# THE RETURN TO ADAPTATION IN A CHANGING CLIMATE

Harrison Hong
Serena Ng
Jiangmin Xu

Working Paper 33824
http://www.nber.org/papers/w33824

NATIONAL BUREAU OF ECONOMIC RESEARCH
1050 Massachusetts Avenue
Cambridge, MA 02138
May 2025, Revised December 2025

We thank Benjamin Olken, Robin Burgess, Maryam Farboodi, Allan Hsiao, Marshall Burke, Adrien Bilal, Mark Watson, Chad Jones, Nobuhiro Kiyotaki, and seminar participants at the London School of Economics Environment Week, Stanford GSB Climate Conference, Columbia University, Econometric Society Meetings (Ho Chi Minh), Insper, Australasian Banking and Finance Conference, Macquarie University, University of Sydney, and Sabanci University (Istanbul) for helpful comments. Ng acknowledges financial support from the National Science Foundation (SES 2018369). Hong acknowledges financial support from a Guggenheim Fellowship. The views expressed herein are those of the authors and do not necessarily reflect the views of the National Bureau of Economic Research.

The Return to Adaptation in a Changing Climate
Harrison Hong, Serena Ng, and Jiangmin Xu
NBER Working Paper No. 33824
May 2025, Revised December 2025
JEL No. O1, O40, O47, Q50, Q54, Q56


## ABSTRACT

We develop a two-step econometric framework to quantify the economic return to adaptation in a changing climate. The approach exploits the time-inhomogeneity of disaster arrivals, which generates learning and time-varying incentives for adaptive investment. First, we estimate country-specific dynamics of perceived disaster risk using a flexible class of time-varying arrival processes. Second, we link these dynamics to the marginal impact of extreme-weather damage on growth. Damage is systematically lower when risk is high—i.e., when disasters arrive in clusters—consistent with risk-dependent adaptation. To identify the expectations mechanism, we show that the return to adaptation is highest in countries where disaster arrivals are most serially correlated or the signal of future strikes is strongest. Absent such adaptation, average national income today would be several percent lower, with the shortfall widening significantly as countries learn about their evolving climate risks. These estimates are robust across various perceived-risk processes with different martingale properties.



Harrison Hong
Columbia University
Department of Economics
and NBER
hh2679@columbia.edu

Jiangmin Xu
Peking University
Department of Finance
jiangminxu@gsm.pku.edu.cn

Serena Ng
Columbia University
Department of Economics
and NBER
Serena.Ng@columbia.edu

# 1 Introduction

The economic impact of extreme weather is unequivocal: A large body of empirical research confirms that cyclones, heatwaves, and other climate-linked shocks significantly damage long-run economic growth (see Dell, Jones, and Olken (2014) for a review).[1] While the consensus on the rising magnitude of global climate risk is strong (National Academies of Sciences, Engineering, and Medicine (2016)), the dynamic role and quantifiable economic return to adaptation remain an open question in both climate economics and policy (Bouwer, Crompton, Faust, Höppe, and Pielke Jr (2007)).

Prior influential work identifies adaptation cross-sectionally—comparing differences in damage between countries based on their fixed historical geographical exposure. For instance, lower damage per tropical cyclone in the Philippines compared to a less-exposed country is attributed to a fixed level of adaptation built up from past experience (Hsiang and Jina (2014); Bakkensen and Mendelsohn (2016)). However, this method relies on time-invariant differences.

In contrast, we propose an alternative framework that identifies adaptation within countries over time, exploiting the fact that extreme-weather risk is time-inhomogeneous in a changing climate. Crucially, there is considerable uncertainty regarding the consequence of global warming for extreme weather. Because societies learn from realized disasters (Sisco, Bosetti, and Weber (2017)), this learning generates risk-dependent adaptation, whereby damages decline when risk is perceived to be high, i.e., when arrivals are clustered.[2] This is a central benefit of our dynamic approach: countries with more predictable or clustered arrivals, and thus greater scope for learning, are precisely where the return to adaptation is expected to be largest.

This approach provides a tighter identification strategy by isolating the effects of risk-dependent adaptation driven by a society's evolving beliefs—a crucial, forward-looking dimension missed by static comparisons. Our empirical design builds on the theoretical insights of Hong, Wang, and Yang (2023), who extend the neoclassical growth model to incorporate learning and adaptation in the presence of rare disasters. We implement a two-step estimation procedure that separates (i) the evolution of country-specific disaster risk from (ii) the damage of extreme weather conditional on that risk.

In the first step, for our baseline specification, we estimate time-varying disaster arrival rates

[1] Economic damages from extreme weather have risen sharply in recent decades. According to the National Oceanic and Atmospheric Administration (NOAA), the United States has experienced 391 billion-dollar disasters since 1980, with CPI-adjusted losses totaling $2.75 trillion.

[2] According to a survey of tropical-cyclone models (Knutson, Camargo, Chan, Emanuel, Ho, Kossin, Mohapatra, Satoh, Sugi, Walsh, et al. (2020)), the median model projects a modest 13% increase in the frequency of major tropical cyclones in a $2^oc$ world relative to pre-industrial era. The most pessimistic climate model projects a two-fold increase, while the most optimistic model projects a slight decrease.

using a two-component mixture of Poisson distributions—one with a high mean and one with a low mean—representing heterogeneity across "good" and "bad" climate states. This mixture formulation captures clustered extreme-weather arrivals without requiring explicit state transitions. Societies update beliefs about this latent state as disasters occur. The evolution of beliefs about the bad state yields a country-specific measure of perceived disaster risk that follows a martingale process. This Bayesian learning interpretation is consistent with the observed volatility clustering in extreme-weather risk.

In the second step, we relate economic damages from extreme weather to these estimated, time-varying risks. If adaptation is effective, damages should fall when perceived risk is high—that is, during periods of clustered disaster arrivals, society should be more prepared. The estimated interaction between damages and risk quantifies the return to adaptation. Moreover, this return should be larger in countries where the risk process is more non-i.i.d.—that is, where arrivals are more serially correlated or there is more volatility clustering—allowing us to rule out non-expectations-based explanations such as "vintage" effects of adaptation and strongly supporting the learning mechanism.

As alternatives to our baseline mixture model, we also estimate deterministic time-trend specifications for disaster arrivals, allowing for linear and nonlinear trends in the Poisson intensity. These models capture smoother shifts in the mean arrival rate rather than Bayesian updating. The mixture model with Bayesian updating provides the structural interpretation of risk as a martingale, whereas trend-based models can be viewed as sub- or super-martingales. Comparing results across the mixture and deterministic models allows us to assess the sensitivity of the return to adaptation to the martingale properties of time-varying risk processes.

We apply this framework to global panels of tropical cyclones and extreme temperatures from 1980–2019 (as in Dell, Jones, and Olken (2012); Hsiang and Jina (2014)). Our findings are as follows. First, we reject a time-invariant Poisson model in favor of time-varying arrivals: extreme-weather shocks increase the likelihood of subsequent events. Second, we find strong evidence of state-dependent adaptation—economic damages that decline when disaster risk is high, consistent with learning and adaptive investment.

Third, controlling for the prior risk of a country, the return to adaptation is larger in countries where arrivals are the most serially dependent and the signal of future strikes is the greatest. This finding identifies the learning mechanism and the adaptation driven by expectations. Our exclusion restriction is that the cross-country heterogeneity in the serial correlation of arrivals, after adjusting for prior risk, is uncorrelated with other attributes of countries that might also determine damage from arrivals. On the plausibility of the exclusion restriction, the extent to which there is clustering of arrivals in the data is uncorrelated with measures of country-level

economic development.

Fourth, counterfactuals indicate that without such adaptation, average national income in 2019 would have been 6.5% lower for cyclone-exposed countries and 4% lower for those facing heat extremes. Fifth, we use SSP5 growth projections (Kriegler, Bauer, Popp, Humpenöder, Leimbach, Strefler, Baumstark, Bodirsky, Hilaire, Klein, et al. (2017)) to assess long-run adaptation returns. By 2050, mean income would be roughly 13-15% lower if damages remained fixed at prior risk levels. The value of adaptation thus scales strongly with the resolution of uncertainty about climate risk over time.

Finally, our empirical findings on the return to adaptation are robust to the martingale properties of underlying perceived risk processes. This might seem surprising at first. However, despite differences in the martingale properties, forecasts from both approaches are highly correlated over long horizons, thus leading to similar estimates and projections.

Our paper contributes in three ways. (1) We provide the first empirical framework that jointly estimates the evolution of disaster risk and state-dependent damages, allowing adaptation to vary endogenously over time and hence extending the empirical specifications in earlier influential work by Dell, Jones, and Olken (2012). (2) We show that disaster arrivals themselves carry information that shapes future adaptation incentives, highlighting the crucial role of learning and predictable risk clustering in driving adaptation returns. (3) We quantify both the short-run and long-run returns to adaptation, with implications for dynamic welfare and integrated assessment models (Nordhaus (2017); Golosov, Hassler, Krusell, and Tsyvinski (2014); Barnett, Brock, and Hansen (2020)).

By embedding dynamic, Bayesian learning directly in the estimation of disaster risk, our approach recovers how societies adapt as uncertainty about extreme weather resolves. This forward-looking perspective, rather than relying on fixed prior experience, is essential for quantifying the full economic value of climate resilience.

# 2 Data

We consider two widely-studied extreme-weather events in the literature: tropical cyclones and abnormal temperatures. We first describe the data in Section 2 and then present some key stylized facts in Section 3 to motivate the importance of integrating time-varying extreme-weather risk as a state variable into estimation of economic damages.

**Tropical cyclones.** Our data comes from the International Best Track Archive for Climate Stewardship (IBTrACS) database. It is the most complete global database for tropical cyclone

observations. Our largest sample contains annual observations for the real GDP per capita growth rate and cyclone landfalls across 109 countries from 1980 to 2019 with 4,264 country-year observations in total.[3] This is the same set of countries and places as in Hsiang and Jina (2014), but excludes Taiwan for which there is no GDP data from the World Bank Development Indicators. For countries covering large areas — such as the U.S., China, and Canada, we consider data only from the eastern regions that are the most prone to cyclone landfall to avoid any potential bias that might arise if we include large areas mostly unaffected by cyclones. Let $\text{Landfall}_{i,t}$ be an indicator variable that equals one if and only if country $i$ experienced at least one cyclone landfall that is "tropical storm" or higher in year $t$.

To concisely summarize the data, we assign the 109 countries into four regions: North Atlantic (including North America, the Caribbean, and West Europe), West Pacific (including Oceania), North India (including North India, Middle East, North Africa, and Central Europe), and South Atlantic (including Latin America and Sub-Saharan Africa). Globally, a country experiences a tropical cyclone landfall once every 7.4 years on average, as the disaster arrival rate is 0.135 per annum. There is variation across regions, with West Pacific countries getting hit more frequently (at a rate of 0.515 per annum).

**Temperature.** Our temperature panel contains annual observations of temperature across 139 countries from the year 1980 to 2019, similar to the one used in Dell, Jones, and Olken (2012) and Burke, Hsiang, and Miguel (2015).[4] The data, which come from Willmott and Matsuura (2018), contain 0.5 degree gridded monthly average temperature for all land areas over the period 1900-2017. Data for 2018 and 2019 are taken from Berkeley Earth.[5] As in Burke, Hsiang, and Miguel (2015), we first aggregate the 0.5 degree grid cell temperature values to the country-month level, weighting by population density in the year 2000 using data from the Gridded Population of the World hosted by CIESIN at Columbia University.[6] Then we aggregate to the country-year level by averaging monthly values across all months in a year for each country. We define a country as being hit by heatwaves if the mean summer temperature is, relative to historical summer norms, above $1^o$C.[7]

[3] We use pre-1980 data, from 1960-1979, to inform the prior beliefs.

[4] Our temperature sample starts in 1980 so as to overlap with our cyclone sample and with economic data. Another reason is that data from recent decades are more likely to be informative about the consequences of climate change than data from earlier decades (see Section 5.1). We use pre-1980 data, from 1960-1979, to set the prior beliefs.

[5] Data source: `http://berkeleyearth.org/`.

[6] See Gridded Population of the World (GPW), v3, `https://sedac.ciesin.columbia.edu/data/collection/gpw-v3`.

[7] Heatwaves occur in the summer and can last anywhere from days to weeks. We will refer to heatwaves and an extremely hot summer interchangeably.

Table 1: Summary statistics of extreme weather data, 1980:2019

This table shows the summary statistics of cyclone (Panel A) and extreme temperature arrivals (Panel B) for our sample of global countries. The regions for cyclone in Panel A are: North Atlantic (including North America, the Caribbean, and West Europe), West Pacific (including Oceania), North India (including North India, Middle East, North Africa, and Central Europe), and South Atlantic (including Latin America and Sub-Saharan Africa). The regions for heatwaves in panel B are: (1) EUNA: Europe and North America, (2) ASME: Asia, Middle East and North Africa, (3) CLAC: Caribbean and Latin America, and (4) SSAF: Sub-Saharan Africa.

Panel A: Cyclone arrival frequency

| Region | (1) Total # of country-year obs. | (2) Total # of cyclone landfall obs. | (3) Freq. of landfall = (2)/(1): Disaster arrival intensity $\lambda$ |
|---|---|---|---|
| North Atlantic | 1249 | 181 | 0.145 |
| West Pacific | 501 | 258 | 0.515 |
| North India | 561 | 52 | 0.093 |
| South Atlantic | 1953 | 82 | 0.042 |
| Global | 4264 | 573 | 0.134 |

Panel B: Heatwave arrival frequency

| Region | (1) Total # of country-year obs. | (2) Total # of heatwave disaster obs. | (3) Freq. of heatwave = (2)/(1): Disaster arrival intensity $\lambda$ |
|---|---|---|---|
| EUNA | 1319 | 298 | 0.226 |
| ASME | 1431 | 284 | 0.198 |
| CLAC | 1031 | 249 | 0.242 |
| SSAF | 1742 | 382 | 0.219 |
| Global | 5523 | 1213 | 0.220 |

For this data, we classify countries into the following regions: (1) EUNA (Europe and North America), (2) ASME (Asia, Middle East and North Africa), (3) CLAC (Caribbean and Latin America), and (4) SSAF (Sub-Saharan Africa).[8] Panel B of Table 1 shows the summary statistics of summer extreme temperature of 1.0°C+ in each global region in our sample. The typical country faces an arrival rate of 0.22 or is hit by a summer extreme temperature once every 5 years or so.

**Economic Data.** The key economic indicators of interest are the growth rate of real GDP per capita ($g$), investment ratio ($i$) (to lagged output), depreciation rate ($\delta$), and Tobin's $q$. Tobin's (average) $q$ is calculated using the market value of the stock market of that country divided by the book value of capital stock of that country. In addition, we calculate the GDP growth rate net of the difference between the investment and depreciation rates ($g - (i - \delta)$), as it will be the natural variable of interest according to our model of the impact of extreme weather on the macroeconomy.

These economic variables are constructed using COMPUSTAT and World Bank data sources. Panel A of Table 2 reports the mean of the economic data for the cyclone sample. The mean GDP growth rate is 1.75% (st.dev. of 4.8%). The mean investment ratio is 0.21 (st.dev. of 0.08). The mean Tobin's $q$ is 2.45 (st.dev. of 4.70). The net GDP growth rate has a mean of -0.17 with a standard deviation of 0.26, suggesting that investment net of depreciation is an important driver of GDP growth. As seen in Panel B of Table 2, the means of the economic indicators for the extreme temperature sample are comparable to that for the cyclone sample.

# 3 Stylized Facts

We start with a constant-coefficient linear panel regression model that is widely used to estimate the impact to an economic outcome $Y_{it}$ from extreme-weather arrivals (see, e.g., Dell, Jones, and Olken (2014)):

$$Y_{it} = \phi D_{it} + u_i + v_t + \varepsilon_{it}, \tag{1}$$

where $D_{it}$ is an indicator variable that equals 1 when country $i$ is hit by an extreme event in year $t$. In the literature, the main dependent variable of interest $Y_{it}$ is typically GDP growth

[8] In Dell, Jones and Olken (2012), there are 6 regions in total, with a separate Middle East & North Africa and an Eastern Europe & Central Asia region. Since the number of observations in the separate Middle East & North Africa and Eastern Europe & Central Asia regions are small, we merge these two regions with other bigger regions to have a more balanced number of observations in each region. We merge the Middle East & North Africa region with the Asia region to form our region (2), and assign the countries in the Eastern Europe & Central Asia region to our region (1) and (2) accordingly, so we have 4 regions in total.

Table 2: Summary statistics of economic variables

This table shows the summary statistics of the economic variables for our sample of global countries. Panel A and B show the summary statistics for the cyclone and heatwave samples respectively. GDP denotes growth rate of real GDP per capita (in percentages). Investment ratio denotes investment scaled by lagged output. GDPnet denotes GDP growth net of $(i_{t-1} - \delta)$ (lagged investment rate minus depreciation). Tobin's $q$ denotes market value of equity market divided by book value of capital. The sample is from 1980 to 2019.

| Panel A: Cyclone | | | | | |
|---|---|---|---|---|---|
| | Mean | S.D. | Median | P10 | P90 |
| GDP (%) | 1.75 | 4.80 | 2.11 | -3.56 | 6.53 |
| Investment ratio | 0.21 | 0.08 | 0.20 | 0.12 | 0.31 |
| GDPnet (%) | -0.17 | 0.26 | -0.13 | -0.45 | 0.06 |
| Tobin's $q$ | 2.45 | 4.70 | 1.50 | 0.61 | 3.65 |

| Panel B: Heatwave | | | | | |
|---|---|---|---|---|---|
| | Mean | S.D. | Median | P10 | P90 |
| GDP (%) | 1.65 | 5.96 | 2.02 | -3.71 | 6.68 |
| Investment ratio | 0.22 | 0.08 | 0.21 | 0.13 | 0.32 |
| GDPnet (%) | -0.18 | 0.30 | -0.15 | -0.53 | 0.08 |
| Tobin's $q$ | 2.33 | 3.95 | 1.51 | 0.64 | 3.52 |

of a country. The regression includes $u_i$ a country fixed effect and $v_t$ a time fixed effect.[9] Thus in this linear model (1), the coefficient $\phi$ captures the impact of an extreme event on economic outcome $Y_{it}$.

In Table 3, we report results for four definitions of outcome $Y_{it}$: GDP growth, aggregate investment, Tobin's $q$, and scaled future extreme-weather arrivals. In column (1), we report the impact of an extreme event for GDP growth that is adjusted for investment and depreciation. The coefficient of interest is -0.916 with a t-statistic of -5.04 for tropical cyclones and -0.767 with a t-statistic of -4.11 for heatwaves. The economic effect of an extreme-weather event for a typical country in our sample is quite adverse — lowering economic growth by 77 to 92 bps. These are well-known findings in the literature.

In columns (2) and (3), we consider the investment-to-lagged output ratio and Tobin's $q$ as the dependent variables of interest. We find that there is also a pronounced decline in both investment and Tobin's $q$. This set of findings (columns (2)-(3)) are inconsistent with a neoclassical model of investment with time-invariant arrival rate of disasters (Pindyck and Wang (2013)). To see why, first observe that the arrival of a disaster destroys capital stock, which of course leads to a drop in contemporaneous growth rate of output. However, investment and

[9] Alternatively, the literature sometimes replaces the time fixed effect with a region × time fixed effect.

Table 3: Panel regressions of economic variables on extreme weather arrivals

This table shows the result from a baseline climate-economy panel regression that regresses an economic variable on an indicator for extreme weather events (tropical cyclone or heatwave arrivals). Panel A shows the cyclone sample results while Panel B shows the heatwave sample results. The dependent variables are GDP growth net of $(i_{t-1} - \delta)$ (column 1), investment ratio (scaled by lagged output) (column 2), Tobin's q (column 3), and scaled future arrival, defined as the number of future arrivals in a 3-year bin from $t+1$ to $t+3$ divided by 3 (column 4). The main explanatory variable is the extreme weather arrival indicator at $t$, i.e., $D_t$. We control for country fixed effects and year fixed effects in all regressions. $t$-statistics with clustered robust standard errors are shown in parentheses below the estimates. ***, **, and * denote statistical significance at the 1%, 5%, and 10% levels respectively. The sample is from 1980 to 2019.

| Panel A: Cyclone | | | | |
|---|---|---|---|---|
| | (1) GDPnet | (2) Investment ratio | (3) Tobin's $q$ | (4) Future arrivals |
| $\hat{\phi}$ | -0.916*** | -1.005*** | -0.107** | 0.036** |
| | (-5.04) | (-4.12) | (-2.29) | (2.50) |
| Country FE | Yes | Yes | Yes | Yes |
| Year FE | Yes | Yes | Yes | Yes |

| Panel B: Heatwave | | | | |
|---|---|---|---|---|
| | (1) GDPnet | (2) Investment ratio | (3) Tobin's $q$ | (4) Future arrivals |
| $\hat{\phi}$ | -0.767*** | -0.855*** | -0.172*** | 0.078*** |
| | (-4.11) | (-3.59) | (-2.86) | (3.14) |
| Country FE | Yes | Yes | Yes | Yes |
| Year FE | Yes | Yes | Yes | Yes |

Tobin's $q$ are forward looking variables. If agents in the economy perceive the risk of extreme weather as being unchanged, then they should not change their investment plans and Tobin's $q$ should be unchanged. If anything, a disaster that destroys capital should mechanically lead to a higher investment-to-output ratio.

In column (4) the dependent variable $Y_{it}$ is the number of extreme-weather arrivals for country $i$ in a 3-year bin from $t+1$ to $t+3$ divided by 3, i.e. $Y_{it} = \frac{1}{3}(D_{it+1} + D_{it+2} + D_{it+3})$. We find that the arrival of an extreme-weather event is also associated with the country experiencing more frequent strikes over the next three years. That is, the risk of extreme-weather events is time-varying and persistent. Hence, to simultaneously rationalize columns (1)-(4) one can model time-varying disaster risk so that agents learn as this risk varies. The reason investment and Tobin's $q$ are lower following a disaster is that agents in the economy perceive extreme-weather risk as being elevated. Rather than investing, society presumably shifts those resources to costly adaptation to better protect capital.

Papers in the empirical literature on damages to GDP growth do not explicitly model time-varying risk (see further discussion in Section 4.2). As such, we now turn to a state-dependent approach to modeling damages to economic growth, which can help us improve on the empirical specifications used in the literature. We are particularly focused on developing empirical specifications that allow us to estimate the return of adaptation to extreme weather.

# 4 Extreme-Weather Damages: Theory and Estimation

Our empirical approach builds on a couple of key features of Hong, Wang, and Yang (2023), who generalize the neoclassical growth model to allow optimizing agents to adapt to disasters. In their continuous-time model, an economy (subsequently indexed by $i$, and suppressed in this subsection to simplify notation), disasters arrive according to a Poisson process with intensity $\lambda$ which can take on one of two values: $\lambda_G$ (good) or $\lambda_B$ (bad), with $\lambda_B > \lambda_G$.The representative agent (of economy $i$) has a prior belief $\pi_0$ that the true value of $\lambda$ is $\lambda_B$. At each $t$, the agent forms a posterior belief $\pi_t = P_t(\lambda = \lambda_B)$ based on observed signals, where $P_t(\cdot)$ is the conditional probability at $t$. A higher value of $\pi_t$ corresponds to a belief that state B is more likely. The expected disaster arrival rate at $t$ given $\pi_t$ is

$$E_t(\lambda; \pi_t) = \lambda_B \pi_t + \lambda_G(1 - \pi_t)$$

Signals arrive in the form of jumps $d\mathcal{J}_t$, which equals one if there is a disaster and zero otherwise.[10] Given a pre-jump belief of $\pi_{t-}$, belief evolves according to $d\pi_t = \sigma_\pi(\pi_{t-})(d\mathcal{J}_t - \lambda_{t-}dt)$. Specifically, after a disaster at $t$, beliefs change in an unfavorable way to

$$\pi_t^{\mathcal{J}} = \pi_{t-} + \sigma(\pi_{t-}) = \frac{\pi_{t-}\lambda_B}{E_t(\lambda_t; \pi_{t-})} > \pi_{t-}. \tag{2}$$

where $\sigma(\pi_{t-}) = \frac{\pi_{t-}(1-\pi_{t-})(\lambda_B - \lambda_G)}{\lambda(\pi_{t-})}$ is the size of the jump (i.e. revision in prior) with the arrival of an event. If there is no arrival over interval $dt$ (i.e. $d\mathcal{J}_v = 0$ for $v \in (s, t)$), then beliefs evolve according to a logistic differential equation $\frac{d\pi_t}{dt} = -\sigma_\pi(\pi_{t-})E_t(\lambda; \pi_{t-})$ whose closed-form

[10]Note that if the number of arrivals per interval of time is Poisson distributed, the length of time between occurrences has an exponential distribution.

solution is given by

$$\pi_t^{\mathcal{NJ}} = \frac{\pi_s \exp\Big( -(\lambda_B - \lambda_G)(t-s)\Big)}{1 + \pi_s\Big[\exp\Big( -(\lambda_B - \lambda_G)(t-s)\Big) - 1\Big]}.$$

Their model predicts that agents will adapt to disasters, in the sense that economic outcomes (such as economic growth, Tobin's $q$ and equity risk premium) will be different from the case when there is no learning. For example, output growth $g_t$ (adjusted for investment and depreciation) will take the form

$$g_t = (i(\pi_{t-}) - \delta)dt + F(\pi_{t-})dJ_t + \sigma dW_t. \tag{3}$$

where $i$ is the investment-to-capital ratio, $\delta$ is the depreciation rate, $F(\pi_{t-})$ is an adaptation function that mediates damage to growth caused by the jump $dJ_t$ and depends on beliefs $\pi_t$, and $dW_t$ is an idiosyncratic Brownian shock. The output response to disasters ($dJ_t = 1$) is state-dependent with two features: it is time varying (to the extent that $\pi_{t-}$ varies with $t$) and possibly non-linear (to the extent that $F(\cdot)$ is non-linear). As $\pi_{t-}$ rises, there is more adaptation spending which lowers economic damage.

## 4.1 Estimating Time-Varying Extreme-Weather Risk

Both features of the model can be seen by simulating the model in discrete time given country-specific parameters $\theta = (\lambda_B, \lambda_G)$. We initialize $\bar{\lambda}_0 = \pi_0\lambda_B + (1-\pi_0)\lambda_G$ with $\pi_0$ set to a country's 1960-1979 mean arrival rate. For $t > 1$, we simulate a Poisson jump arrival based on the mean $\bar{\lambda}_{t-1} = \lambda_B\pi_{t-1} + \lambda_G(1-\pi_{t-1})$. Defining $D_t = 1$ when an arrival occurs, posterior beliefs are updated as[11]

$$\pi_t = \begin{cases} \dfrac{\pi_{t-1}\lambda_B}{\pi_{t-1}\lambda_B + (1-\pi_{t-1})\lambda_G} & \text{if} \quad D_t = 1 \\ \dfrac{\pi_{t-1}\exp(-(\lambda_B - \lambda_G))}{1 + \pi_{t-1}[\exp(-(\lambda_B - \lambda_G)) - 1]} & \text{if} \quad D_t = 0\ . \end{cases} \tag{4}$$

Since countries are heterogeneous, we simulate one model for each country $i = 1, \ldots, N$. Though the true country-specific parameters $\{\theta_i^0\}_{i=1}^N$ are unknown, we have data on extreme

[11] See also Lipster and Shiryaev (2001, Theorem 19.6) for optimal filtering of point processes, and Example 1 on p.333.

weather events $D_i = (D_{i1}, \ldots, D_{iT})'$ from which we can compute sample moments $\hat{\psi}(D_i, \theta_i^0)$ for each $i$. Assuming that the binding function $\psi(\cdot)$ is invertible, we can estimate $\theta_i$ country-by-country using moments $\bar{g}_i = \hat{\psi}(D_i, \theta_i^0) - \hat{\psi}(\theta)$ whose asymptotic variance $\Omega_i$ can be consistently estimated by $\hat{\Omega}_i$. As $\psi(\cdot)$ is not tractable, we approximate it by simulations. Let $\hat{\psi}^S(\theta) = \frac{1}{S}\sum_{s=1}^{S} \hat{\psi}(D_i^s, \theta)$ be the moments computed from data $D_i^s$ simulated under $\theta$ using the $s$-th draw of errors, $s = 1, \ldots, S$. Let $\bar{g}_i^S = \hat{\psi}(D_i, \theta_i^0) - \hat{\psi}^S(\theta)$. Under regularity conditions in (Duffie and Singleton (1993)), the simulated method of moments (SMM) estimator $\hat{\theta}_i^S = \text{argmin}_\theta \bar{g}_i^S(\theta)' \hat{\Omega}_i^{-1} \bar{g}_i^S(\theta)$ is root-$T$ consistent and asymptotically normal.

## 4.2 Estimating Risk-Dependent Damages

A widely-used approach to estimating the value of adaptation to disasters such as tropical cyclones (Bakkensen and Mendelsohn (2016), Hsiang and Jina (2014)) is to measure how economic damage conditional on a disaster arrival significantly declines cross-sectionally with the historical experience of a locale with disasters (see, e.g., Dell, Jones, and Olken (2014) for a review).[12] They augment the linear model (1) for GDP growth by estimating the following panel regression:

$$g_{it} = \phi D_{it} + (\psi \cdot n_i) \times D_{it} + u_i + v_{jt} + \varepsilon_{it}, \tag{5}$$

where $n_i$ is the variable measuring the number of extreme weather events a country $i$ has experienced historically, $u_i$ is a country fixed effect, and $v_{jt}$ is a region-by-time fixed effect. Adaptation studies typically find that $\psi$ is negative, i.e., countries with more extreme weather arrivals historically (measured by high $n_i$ values) would experience lower damage for an given event $D_{it}$. Thus in this reduced-form model (5), the coefficient $\phi$ captures the conditional damage without adaptation and the coefficient $\psi$ captures the adaptation effect. This time-invariant approach is a special case of our setting when we assume that there is no learning, i.e. the level of adaptation is fixed at prior risk levels.

Locales or countries with more prior experience are found to have less damage per disaster, consistent with adaptation. Studies examining the value of adaptation for temperature also utilize aspects of this approach (Auffhammer (2022), Gourio and Fries (2020), Carleton, Jina, Delgado, Greenstone, Houser, Hsiang, Hultgren, Kopp, McCusker, Nath, Rising, Rode, Seo, Viaene, Yuan, and Zhang (2022)).[13]

[12] This time-invariant approach, which goes back to earlier work on identifying the impact of temperature on agricultural yields (Deschênes and Greenstone (2007) and Schlenker and Roberts (2009)), relies on location and time fixed effects to address unobserved heterogeneities in the panel data.

[13] An exception is Bilal and Känzig (2024) who use aggregate (global) time-series variation to measure economic damages from changing average temperatures.

Though simple and intuitive, there are several limitations to this regression. While the model allows for heterogeneity through individual and time fixed effects, a linear model with time constant parameters would not encompass the possible effects of learning and risk-dependent adaptation, which as we have pointed out in Section 3 are likely.[14] And when the coefficients are heterogeneous, pooled estimation has its drawbacks. As reviewed in Baltagi (2008) in the context of linear models, if the slope parameters are homogeneous, pooling is efficient when $N$ is large and $T$ is small. But pooling becomes less appealing when the slope coefficients are heterogeneous especially in the presence of dynamics. Pesaran and Smith (1995) showed that the average effect will be inconsistent if the omitted heterogeneity induces a correlation between the serially correlated regressors and the regression error.

An alternative to pooling is unit by unit estimation which will yield consistent estimates when $T$ is large. Arguably, we have enough disaster observation for each country to consider individual level estimation. The main appeal is that there is more flexibility to estimate a model with the desired state-dependent effects at the country level. After country-by-country regressions, we can still compute the average. In other words, we solely utilize the time series of a country to identify the return to risk-dependent adaptation, whereas the literature uses cross-locale variation in prior risks or disaster experiences to value adaptation.

Equation (3) suggests a flexible alternative to the linear model

$$g_{it} - (i_{it-1} - \delta_{it-1}) = \mu_i + F(\pi_{it-1})D_{it} + \varepsilon_{it}, \tag{6}$$

where $F(\pi_{it-1})$ is the adaptation-induced damage function. Rather than modeling the growth rate $g_{it}$, we will instead work with GDP growth net of the difference between the investment rate and depreciation rate, i.e. $g^n_{it} = g_{it} - (i_{it-1} - \delta_{it-1})$. That is, we will net out the previous level of investment and also adjust for depreciation to give us a mean zero dependent outcome. Note that all variables in the regression are country-specific. The linear model in Equation 1 obtains as a special case when $F(\pi_{it-1})$ is a constant $\zeta_{1i} = F(\pi_{i0})$, i.e. when there is no learning. Then

$$g^n_{it} = \mu_i + \zeta_{1i}D_{it} + \varepsilon_{it}. \tag{7}$$

The growth of an economy depends on investment (based on $\pi_{it-1}$). We expect the constant term $\mu_i$ to be zero (see also the discussion in Section 2).

If we were only interested in a 'ghat' that allows for time-varying parameters, we could use a non-parametric model (such as a kernel, a neural-net, or a random forest) with $\hat{\pi}_{it}$ and $D_{it}$

[14]Moreover, Barreca, Clay, Deschenes, Greenstone, and Shapiro (2016) document a declining relationship over time in temperature-mortality relationship due to increasing adaptation in the form of air conditioning.

as predictors. But we are interested in the marginal effects of learning and adaptation, so the 'beta-hat' is of interest. We use a first-order Taylor expansion of $F(\pi_{it-1})$ around $\pi_{i0}$ to obtain

$$\begin{aligned} g_{it}^n &= \mu_i + \underbrace{F(\pi_{i0})}_{\substack{\text{damage at} \\ \text{prior adaptation}}} D_{it} + \underbrace{F'(\pi_{i0})(\pi_{it-1} - \pi_{i0})}_{\substack{\text{return to risk-dependent} \\ \text{adaptation}}} D_{it} + \varepsilon_{it} \\ &= \mu_i + \beta_{1i} D_{it} + \beta_{2i} \tilde{\pi}_{it-1} D_{it} + \varepsilon_{it} \\ &= \mu_i + \chi_{it} + \varepsilon_{it} \end{aligned} \tag{8}$$

where $\tilde{\pi}_{it-1} = (\pi_{it-1} - \pi_{i0})$ and $\chi_{it} = \beta_{1i} D_{it} + \beta_{2i} \tilde{\pi}_{it-1} D_{it}$ is the total damage in the presence of learning and adaptation. The $F(\pi_{i0})$ term is economic damage with adaptation fixed at prior risk $\pi_{i0}$. The $F'(\pi_{i0})\tilde{\pi}_{it-1}$ term is the return to risk-dependent adaptation induced by learning or revision of beliefs, which is net of the costs of adaptation to society.

Note that $F(\pi_{i0})$ and $F'(\pi_{i0})$ suffice for identifying the first-order effects of $D_t$, being

$$E[g_{it}^n | D_{it} = 1] = \underbrace{F(\pi_{i0})}_{\beta_{1i}<0} + \underbrace{F'(\pi_{i0})}_{\beta_{2i}>0} \tilde{\pi}_{it-1} \tag{9}$$

The constraints $\beta_{1i} < 0$ and $\beta_{2i} > 0$ will be imposed in estimation. Equation (8) nests the linear model (7) in which $F$ is constant (no risk-dependent adaptation) and $(\pi_{it-1} - \pi_{i0}) = 0$ (no learning). Equation (8) also nests (5) in which $D_{it}$ is not interacted with past beliefs, $\pi_{it-1}$. Omitting dependence on $\pi_{i0}$ and $\pi_{it-1}$ could bias the estimates of economic damages.

# 5 Time-Series Dynamics of Extreme-Weather Risk

## 5.1 First-Stage Estimates

For a given definition of extreme weather (which can be cyclone or extreme temperature), the structural parameters of the model in Section 4 are $\theta = (\lambda_B,\ \lambda_G)'$. Countries' $\pi_0$ values are fixed to their pre-1980 historical extreme-weather arrival frequencies. From Table 4, for tropical cyclones, the mean of $\hat{\pi}_0$ is 0.33 and the median is 0.2. For heatwaves, the mean of $\hat{\pi}_0$ is 0.11 and the median is 0.05. Countries standing in 1980 face a greater prior risk from cyclones than heatwaves.

We estimate $\theta_i$ for each country $i = 1, \ldots, N$ by simulated method of moments. The five sample moments matched to the model are the mean (M1), variance (Var), 3rd central moment (M3), 4th central moment (M4), and first-order autocorrelation (AC). The country-specific

moments are given in Table O.1 and O.2 of the Online Appendix. As we alluded to in Section 2, we are using only the recent four decades of data to discipline our time-varying risk model. We think this is a reasonable choice since the recent decades are likely to be more informative about a changing climate than data early in the twentieth century.

The estimates of $\theta_i$ are summarized in Table 4. For the tropical cyclone sample in Panel A, the mean of $\hat{\lambda}_{Bi}$, the estimated arrival rate in the bad state, is 0.84 (or once in every 1.2 years), with 95% of the estimates being significant. The mean estimate of $\lambda_{Gi}$ is 0.16 (or once in every 6.5 years), with 95% of the estimates being significant. For the extreme temperature sample, the mean estimate of $\lambda_{Bi}$ is 0.727, with 98.3% of the estimates being significant. For estimates of $\lambda_{Gi}$, the mean is 0.138 with again 98.3% of the estimates being significant.

Table 4: Estimates of the arrival model

This table shows the summary statistics over all countries of country-level parameter estimates of the time-varying arrival-rate model of extreme weather in Section 4. $\hat{\pi}_{0,i}$ is set to a country's arrival rate in 1960-1979 sample. Estimates for $\lambda_{B,i}$ and $\lambda_{G,i}$, $\hat{\lambda}_{B,i}$ and $\hat{\lambda}_{G,i}$, are from simulated method of moments targeting the five moments over the sample of 1980-2019 as specified in Online Appendix Tables O.1 and O.2. % Sig. in the second column denotes the percentage of country-level estimates that are significant at the 5% level.

| Panel A: Cyclone | | | | | |
|---|---|---|---|---|---|
| | Mean | % Sig. | Median | Min | Max |
| $\hat{\pi}_{0,i}$ | 0.33 | | 0.2 | | |
| $\hat{\lambda}_{B,i}$ | 0.841 | 95.1% | 0.802 | 0.638 | 0.989 |
| $\hat{\lambda}_{G,i}$ | 0.155 | 95.1% | 0.059 | 0.026 | 0.347 |
| **Panel B: Heatwave** | | | | | |
| | Mean | % Sig. | Median | Min | Max |
| $\hat{\pi}_{0,i}$ | 0.11 | | 0.05 | | |
| $\hat{\lambda}_{B,i}$ | 0.727 | 98.3% | 0.731 | 0.639 | 0.933 |
| $\hat{\lambda}_{G,i}$ | 0.138 | 98.3% | 0.136 | 0.023 | 0.199 |

**Cyclones in Fiji and heatwaves in Germany.** To better understand the implications of the time-varying arrival model, Panel A of Figure 1 plots the path of $\hat{\pi}_{it}$ implied by the cyclone model estimated from data for Fiji, along with the actual arrivals of cyclones (the gray bars). In this case, the cluster of arrivals in the 1990s leads the model to shift its posterior to near 1. But the absence of subsequent cyclones until 2013 leads the posterior to shift down to close to 0 in the late 2000s until recently when $\hat{\pi}_{it-1}$ started to shift up again due to another cluster of arrivals.

Panel B performs a similar plot, but using heatwave data for Germany. The path of $\hat{\pi}_{it}$ for Germany's extreme-temperature is quite different. The $\hat{\pi}_{it}$ series stays close to zero until a

cluster of arrivals in the 2000s lead the posterior risk to rise dramatically. In spite of several abnormally hot summers in the late eighties and early nineties, $\hat{\pi}_{it}$ does not shoot up because the prior risk $\pi_{it}$ is close to zero. According to Equation 2, the size of the jump with the arrival of an event is given by $\sigma(\pi_{t-}) = \frac{\pi_{t-}(1-\pi_{t-})(\lambda_B-\lambda_G)}{\lambda(\pi_{t-})}$. Notice that $\sigma(\pi_{t-})$ is nonlinear in $\pi_{t-}$, and equal to 0 when $\pi_{t-}$ equals 0 or 1. When the risk is extremely low or extremely high, the arrival of an event triggers only a small revision in posteriors, i.e. society is already pretty sure that it is at low or high risk. The largest revisions are typically for intermediate values of $\pi_{t-}$.

Figure 1: Arrivals and evolution of $\hat{\pi}_{it}$: two illustrative examples

This figure shows the arrivals and evolution of $\hat{\pi}_{it}$ for two illustrative examples: Fiji with cyclone data (Panel A) and Germany with heatwave data (Panel B). In each example, the path of $\hat{\pi}_{it}$ computed from the fixed prior $\hat{\pi}_{i0}$ is plotted in the solid black line, and the ones from $\hat{\pi}_{i0}\pm$(the standard deviation of arrivals in the pre-1980 period) are plotted in dotted lines. The gray bars indicate years when there is an arrival.

Panel A: Cyclone example, Fiji

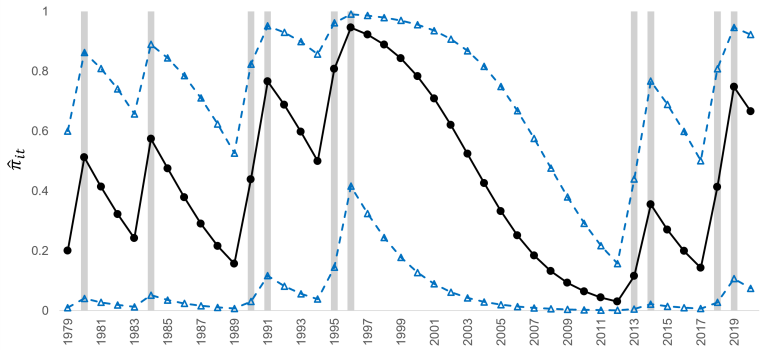


Panel B: Heatwave example, Germany

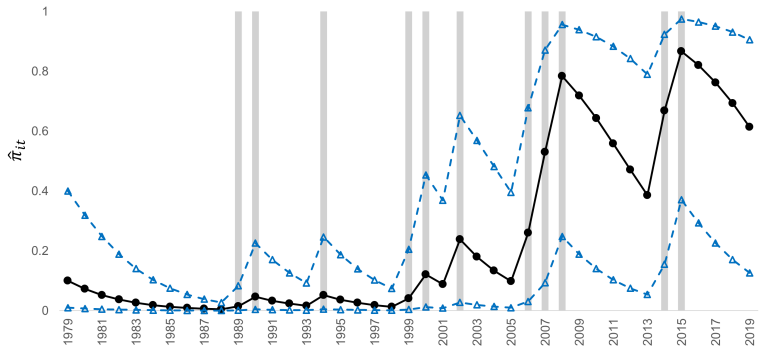


## 5.2 Disaster Arrivals: Constant versus State-Dependent

We first test for adequacy of our 2-parameter (unrestricted) time-varying extreme-weather arrivals model against a restricted time-invariant Poisson arrivals model. This restricted model

Table 5: Test of time-homogeneity of arrivals process: % of countries rejecting null hypothesis $H_0$ at 10 and 5% significance levels

This table presents the summary statistics over all countries of country-level model specification tests for testing the first-stage 2-parameter extreme-weather arrival model versus the restricted simple Poisson arrival model (one constant $\lambda$) estimated using SMM with the five moments specified in Table O.3.

| Model | Equation | $H_0$ | Cyclone | | Heatwave | |
|---|---|---|---|---|---|---|
| | | | 10% | 5% | 10% | 5% |
| Disaster Arrival | (4) | $\lambda_B = \lambda_G$ | 92.8 | 76.8 | 95.0 | 87.6 |

which sets $\lambda_B = \lambda_G$ is also estimated using SMM with the five moments specified in Online Appendix Tables O.1 and O.2. The distance statistic is the difference between the value of the SMM objective function in the restricted Poisson model and our unrestricted extreme-weather arrivals model (both evaluated at their respective SMM estimates) multiplied by $T$. This test statistic has an asymptotic $\chi^2$ distribution with one degree of freedom.

In Table 5, we present the result of this test, which shows the percentage of countries that rejects the null (restricted model). It is clear that for the vast majority of countries, we reject a time-invariant Poisson arrival model of extreme weather in favor of our time-varying arrival rate model at the usual significance levels. For instance, for cyclones, 92.8% of the countries are rejected at the 10% significance level and 76.8% at the 5% significance level. For extreme temperatures, 95% of countries are rejected at the 10% significance level and 87.6% at the 5% significance level.

# 6 Return to Risk-Dependent Adaptation

Having concluded our discussion of the first-stage country risk dynamics, we turn to our second stage estimates. The average effect of economic damages is typically estimated by pooled estimation of a linear model controlling for time and locale fixed effects. We differ in that we allow the damage function to vary with $\pi_{i0}$ and $\pi_{it-1}$, and we impose sign restrictions on the parameters. Furthermore, we perform constrained time series estimation country-by-country, and then aggregate the individual estimates to obtain an estimate of the average effect of interest. The cost to flexibility is that the sample size for the country level regressions is limited by data availability which might affect the estimate of the average effect.

Before turning to non-linear estimation, we want to be confident that our country-by-country approach gives estimates of the average that are similar to panel estimation of the constant parameter linear model $g_{it}^n = \mu + \zeta_{1i} D_{it} + \epsilon_{it}$. To this end, Figure 2 plots the density, estimated

using the Epanchnikov kernel, of the individual $\hat{\zeta}_{1i}$ estimated from the linear model (7). Also shown is the simple average $\hat{\zeta}_1 = \frac{1}{N}\sum_i \hat{\zeta}_{1i}$, as well as the pooled panel estimate $\tilde{\zeta}_1$ (black dotted line). They are $-0.90$ (the average) and $-0.93$ (the pooled) for the cyclone data, and $-0.69$ (the average) and $-0.68$ (the pooled) for the extreme temperature data. We see that $\hat{\zeta}_1$ and $\tilde{\zeta}_1$ are quite similar.

## 6.1 Second-Stage Estimates of the Damage Function

We thus proceed with second-stage estimation of a model with learning and adaptation, i.e.,

$$g_{it}^n = \mu_i + \beta_{1i} D_{it} + \beta_{2i} \tilde{\pi}_{i,t-1} D_{it} + \varepsilon_{it}$$

Figure 2: Density of $\hat{\zeta}_{1i}$

This figure plots the density (estimated using the Epanchnikov kernel) of the individual $\hat{\zeta}_{1i}$ estimated from the linear model (7). The blue solid line is the density. The red dashed line is $\hat{\zeta}_1 = \frac{1}{N}\sum_{i=1}^N \hat{\zeta}_{1i}$. The black dashed line is the estimate of the average effect from a linear panel regression of growth on arrivals with country and region-by-year fixed effects.

Panel A: Cyclone data

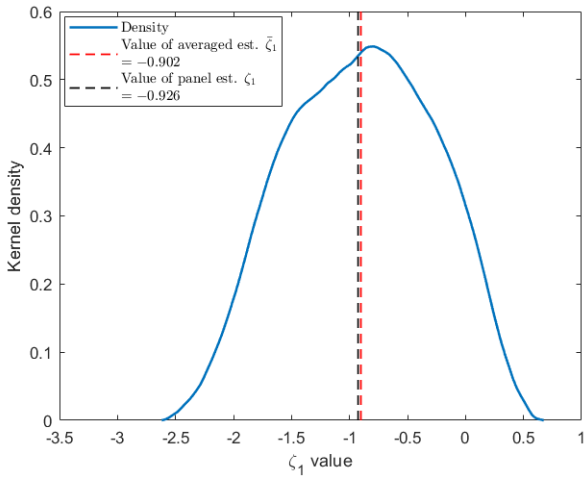


Panel B: Heatwave data

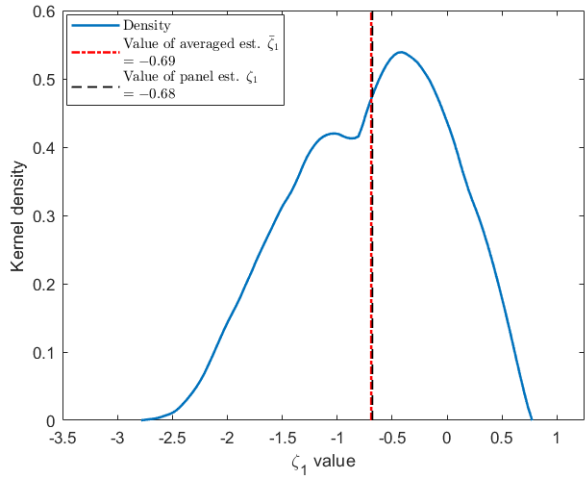


For each country $i$, the damage parameter $\beta_{1i}$ is constrained to be negative and the adaptation parameter $\beta_{2i}$ is constrained to be positive. The density of the estimates are shown in Figure 3. For both the cyclone and extreme temperature data, the density of $\hat{\beta}_{1i}$ is slightly skewed. From $\hat{\beta}_{1i}$ and $\hat{\beta}_{2i}$, we define $\hat{\beta}_1 = \frac{1}{N}\sum_{i=1}^N \hat{\beta}_{1i}$ and $\hat{\beta}_2 = \frac{1}{N}\sum_{i=1}^N \hat{\beta}_{2i}$ and use bootstrap

to obtain their standard errors.[15] We obtain a $\hat{\beta}_1$ of $-0.904$ with a standard error of 0.38 in the cyclone data, and $-0.693$ with a standard error of 0.21 in the extreme temperature data; both significant at the 5% level. Interestingly, $\hat{\beta}_1$ implied by the non-linear model is close to the average estimate $\hat{\zeta}_1$ and the pooled estimate $\tilde{\zeta}_1$ for the linear model shown earlier in Figure 2. However, while a linear model constrains $\beta_{2i}$ to zero, our model with adaptation treats this as a free parameter. The bottom of Figure 3 shows that many of the $\hat{\beta}_{2i}$ are non-zero. The average estimate $\hat{\beta}_2$ is 0.145 with a standard error of 0.06 for the cyclone data, and is 0.126 with a standard error of 0.05 for the extreme temperature data. Both estimates are significant at the 5% level.

To put these estimates into context, the arrival of a cyclone leads to a decline of 90.4 basis points of economic growth for a typical country at its prior risk (the mean $\pi_0$ is 0.3). Suppose that the country's risk increases by 0.5 from its prior, i.e. $(\pi_{t-1} - \pi_0)$ is 0.5, so that its $\pi_{t-1}$ equals 0.8. This would mean that an extreme-weather arrival reduces economic growth only by $0.904 - 0.145 \times 0.5$ or 0.83. In other words, risk-dependent adaptation on net ameliorates damage due to cyclones by 7 basis points.

The benefits of state-dependent adaptation are similar for extreme temperature. For the typical country at its prior risk which is 0.1, the damage to growth from an episode of extreme temperature is 69.3 basis points. If that country's risk rises by 0.5 to 0.6, the damage per arrival of an extreme-weather event falls to 63 basis points. This is a 6.3 basis points reduction.

**GDP growth of Fiji and Germany.** To better understand the variation we are using to isolate $\beta_{2i}$, we return to our Fiji and Germany examples. Figure 4 contains scatter plots of GDP growth (net of $(i_t - \delta)$) against $\hat{\pi}_{it-1}$ at extreme-weather arrival years for our two illustrative country examples. For Fiji, $\hat{\beta}_{1i} = -0.93$ and $\hat{\beta}_{2i} = 0.15$. For Germany, $\hat{\beta}_{1i} = -0.72$ and $\hat{\beta}_{2i} = 0.12$. The positive estimate of $\beta_{2i}$ can be seen from the positive slopes of the scatterplots. The higher is $\hat{\pi}_{it-1}$, the smaller is the damage to GDP growth with an arrival. The coefficient $\beta_{1i}$ is determined by a comparison of these arrival year observations with non-arrival year observations, which are not shown.

[15] Precisely, estimation using the $b$-th bootstrap sample of data for country $i$ gives $\hat{\beta}^b_{1i}$. This yields an average estimate in the $b$-th replication of $\hat{\beta}^b_1 = \frac{1}{N}\sum_{i=1}^{N} \hat{\beta}^b_{1i}$. The standard error of $\hat{\beta}_1$ is estimated by the standard deviation in $\{\hat{\beta}^b_1\}, b = 1, \ldots B$. Similar calculations are performed for $\hat{\beta}_2$.

Figure 3: Density of $\hat{\beta}_{1i}$ and $\hat{\beta}_{2i}$

This figure plots the density (estimated using the Epanchnikov kernel) of the individual $\hat{\beta}_{1i}$ and $\hat{\beta}_{2i}$ estimated from the non-linear model (8). The blue solid line is the density. The red dashed line is the simple average over countries, and the black dashed line is the estimate from a pooled linear regression of growth on arrivals with country and region-by-year fixed effects.

Panel A: Density plot of $\hat{\beta}_{1i}$

Cyclone $\hat{\beta}_{1i}$

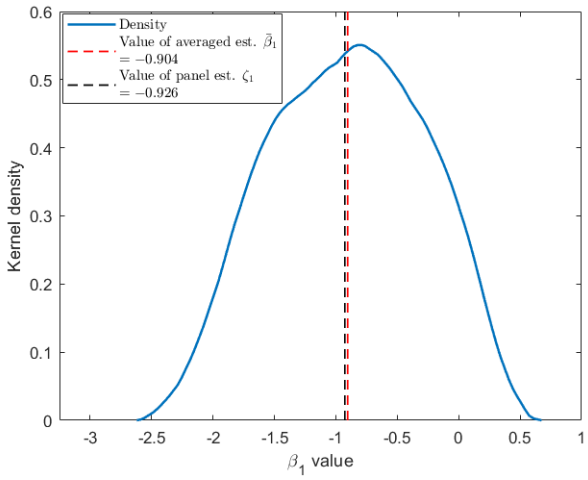


Heatwave $\hat{\beta}_{1i}$

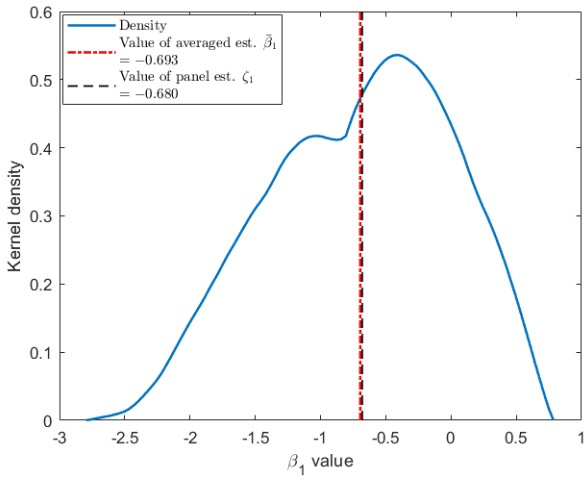


Panel B: Density plot of $\hat{\beta}_{2i}$

Cyclone $\hat{\beta}_{2i}$

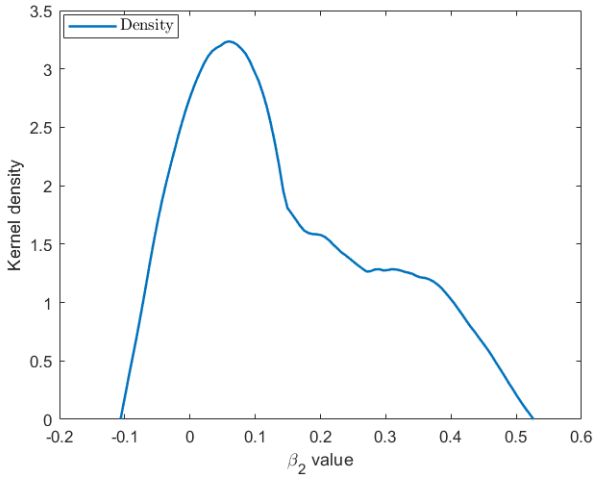


Heatwave $\hat{\beta}_{2i}$

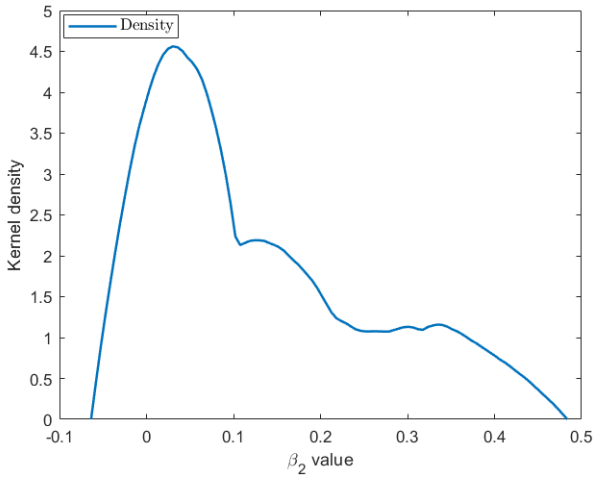

Figure 4: Scatter plots of GDP growth against $\hat{\pi}_{it-1}$ at arrival years, two illustrative examples

This figure scatter plots GDP growth (net of $(i_{t-1} - \delta)$) against $\hat{\pi}_{it-1}$ at extreme-weather arrival years for our two illustrative country examples. For Fiji, $(\hat{\beta}_{1i} = -0.93, \hat{\beta}_{2i} = 0.15)$. For Germany, $(\hat{\beta}_{1i} = -0.72, \hat{\beta}_{2i} = 0.12)$.

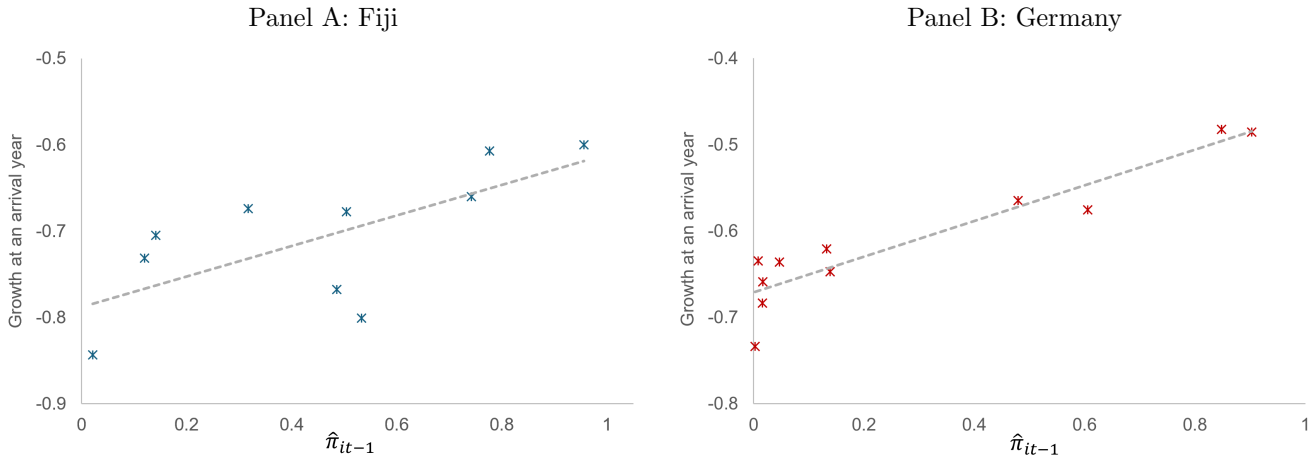


## 6.2 Model Diagnostics

Our approach differs from the approach in the literature in the following dimensions. First, we convert historical weather experience into an extreme-weather risk prior using a Bayesian learning model. Second, we incorporate learning and revision of priors into the country-by-country estimation. This learning term would ordinarily be swept up in the error term. But we show that explicitly accounting for the revisions in priors is important for long-horizon projections. Third, we allow for a nonlinear relationship between adaptation and risk priors. This non-linearity is typically absent in current models which assume that the effect of a disaster arrival on GDP growth is decreasing linearly in arrival experience.

In Appendix A, we provide the following diagnostics to confirm the robustness of our conclusions: (i) a test to show the limitations of linear model used in the second stage; (ii) a residual correlation test for the adequacy of fit from our nonlinear model; (iii) estimates when we consider an aggregate detrending of the data; (iv) panel estimates of our second-stage model.

# 7 Identification of the Expectations Mechanism

A central challenge in empirical adaptation literature is distinguishing true, expectations-driven adaptive behavior from non-expectations-based explanations. For instance, even absent learning, a cluster of disaster arrivals may necessitate the replacement of damaged infrastructure

with newer, more resilient buildings. This pure capital replacement, often termed a "vintage effect," would mechanically reduce subsequent damages, but it is a time-invariant response to realized losses, not a forward-looking investment driven by changing risk perceptions.

To more tightly connect our findings to the learning and expectations mechanism central to our econometric framework, we utilize cross-country variation in the predictability of disaster arrivals, which provides a source of exogenous heterogeneity in the incentive to adapt. When arrivals are highly predictable (i.e., serially correlated), a realized disaster provides a much stronger signal about the current high-risk climate regime, maximizing the returns to immediate, state-dependent adaptation investment. Our baseline mixture model provides a natural structural measure of predictability: the difference between the bad and good state arrival rates, $(\hat{\lambda}_{B,i} - \hat{\lambda}_{G,i})$, which quantifies the magnitude of the regime shift a society is learning about. Recall that $(\hat{\lambda}_{B,i} - \hat{\lambda}_{G,i})$ depends on a number of moments of the arrival process, including the serial correlation AC (see Section 5.1).

## 7.1 Test of Expectations-Driven Adaptation

To the extent society engages in expectations-driven learning, the risk-dependent adaptation parameter $\hat{\beta}_{2i}$ should be larger for countries where the arrivals are more non-i.i.d., controlling for the prior risk of the country $\hat{\pi}_{i0}$. That is, the return to adaptation is highest in environments where the signal of future strikes is strongest.

Table 6: Test of the Expectations-Driven Adaptation

This table shows the cross-sectional regression results of regressing $\hat{\beta}_{2i}$ on $\hat{\pi}_{0,i}$ and $\hat{\lambda}_{B,i} - \hat{\lambda}_{G,i}$. $t$-statistics with bootstrapped standard errors are in parentheses below the estimates, with *** denoting statistical significance at the 1% level.

| Dep Var: $\hat{\beta}_{2i}$ | | |
|---|---|---|
| | Cyclone | Heatwave |
| $\hat{\pi}_{0,i}$ | 0.093 | -0.025 |
| | (1.00) | (-0.15) |
| $\hat{\lambda}_{B,i} - \hat{\lambda}_{G,i}$ | 0.430*** | 0.544*** |
| | (3.46) | (3.61) |

We test this hypothesis in Table 6 by regressing the country-level estimates of the adaptation parameter $\hat{\beta}_{2i}$ on $\hat{\pi}_{0,i}$ and $\hat{\lambda}_{B,i} - \hat{\lambda}_{G,i}$. We find that the return to adaptation $\hat{\beta}_{2i}$ increases with $\hat{\lambda}_{B,i} - \hat{\lambda}_{G,i}$ but has no relationship to prior risk $\hat{\pi}_{i0}$. If the vintage effect were the driving factor, new resilient capital would be built after any disaster, regardless of whether that disaster signaled a high probability of future events.

In Figure 5, we show the scatter plots of country-level second-stage adaptation parameter estimates $\hat{\beta}_{2i}$ (residualized against $\hat{\pi}_{i0}$) against $\hat{\lambda}_{B,i} - \hat{\lambda}_{G,i}$ for both the cyclone and heatwave samples. We find a significant positive relationship in both cases, as indicated by the dashed linear best-fit lines. This result is highly consistent with the learning hypothesis: higher predictability (measured by $(\lambda_{B,i} - \lambda_{G,i})$) points to substantially more pronounced state-dependent adaptations at the country-level. We would obtain the same relationship if we were to use the autocorrelation of disaster arrivals (AC) instead of the structure estimates of the arrival rates.

### 7.2 Exclusion Restriction

The exclusion restriction is that variation in predictability across countries controlling for prior risk is uncorrelated with country attributes that might determine damage from disasters. We provide evidence on the plausibility of our exclusion restriction by examining the correlation between our predictability measures and country-level attributes.

In Table 7, we show cross-sectional correlations of the $\hat{\lambda}_{B,i} - \hat{\lambda}_{G,i}$ estimates and the first-order autocorrelations of arrivals AC (the same as defined in Section 5.1) with a host of standard country-level macroeconomic and financial variables.[16] There is little cross-sectional correlation between these measures of predictability or non-i.i.d.-ness of the arrival process and determinants of economic development, hence giving us reassurance as to the plausibility of our exclusion restriction.

## 8 Counterfactuals

### 8.1 In Sample: 1980-2019

We are interested in comparing the real GDP per capita in 2019 to the counterfactual 2019 income assuming that there had been no learning and state-dependent adaptation over our sample of 1980-2019. We can make this comparison using the actual in-sample GDP growth rates $g_{it}$ for our countries along with estimates of our non-linear time-varying extreme-weather risk model.

[16] We source per capita real GDP (Real GDPpc), inflation rate (Inflation), unemployment rate (Unemployment), current account balance to GDP ratio (Current account to GDP), population growth, and debt to GDP ratio (Debt to GDP) from the World Bank. Moreover, long-term government bond yield (Bond yield) is sourced from LSEG Datastream. For sovereign credit scores (Credit score), we obtain data on sovereign credit ratings from S&P Global, then assign the credit scores 20, 19, 18, ..., 0 to credit ratings AAA, AA+, AA, ..., D respectively. Annual nominal interest rate and stock market data are from the World Bank and the IMF.

Table 7: Correlations of $\hat{\lambda}_{B,i} - \hat{\lambda}_{G,i}$ and AC with macroeconomic and financial variables

This table shows the cross-sectional correlations of the $\hat{\lambda}_{B,i} - \hat{\lambda}_{G,i}$ estimates and AC measures (defined in Section 5.1) with country-level macroeconomic and financial variables. All macro-level variables (except StockVol) for each country are averaged values over the sample period 1980–2019. GDPpc denotes GDP per capita. Bond yield is long-term government bond yield. Credit score is sovereign credit rating score. RealRF is real interest rate. ERP is equity risk premium. Tobin's $q$ is Tobin's average q. StockVol is volatility of annual stock market return.

| | Correlations with $\hat{\lambda}_{B,i} - \hat{\lambda}_{G,i}$ | | Correlations with AC | |
|---|---|---|---|---|
| | Cyclone | Heatwave | Cyclone | Heatwave |
| Real GDPpc | 0.06 | -0.09 | 0.03 | -0.09 |
| Real GDPpc growth | -0.02 | -0.03 | 0.05 | -0.03 |
| Inflation | 0.07 | 0.10 | -0.05 | 0.05 |
| Unemployment | 0.07 | -0.03 | -0.08 | 0.09 |
| Current account to GDP | 0.08 | -0.07 | 0.03 | -0.03 |
| Population growth | -0.03 | 0.09 | -0.02 | 0.08 |
| Debt to GDP | 0.03 | 0.04 | 0.06 | -0.03 |
| Bond yield | 0.07 | 0.11 | -0.11 | 0.12 |
| Credit score | 0.06 | -0.06 | 0.05 | -0.07 |
| RealRF | 0.11 | 0.12 | -0.06 | 0.06 |
| ERP | -0.05 | -0.14 | -0.04 | 0.08 |
| Tobin's $q$ | 0.04 | 0.02 | -0.08 | 0.02 |
| StockVol | -0.10 | -0.08 | -0.09 | 0.13 |

The counterfactual GDP per capita in each year of our sample is:

$$GDP_{it}^{CF} = GDP_{it-1}^{CF} \times (1 + g_{it} - \hat{\beta}_{i2}\tilde{\pi}_{it-1}D_{it}), \tag{10}$$

where $GDP^{CF}$ denotes the counterfactual real $GDP$ per capita, $\tilde{\pi}_{it-1} = (\pi_{it-1} - \pi_{i0})$ and $D_{it}$ equals 1 if the country is hit by a disaster and zero otherwise.[17] $\hat{\beta}_{i2}$ is from our estimates summarized in Figure 3. Equation 10 is a recursive relationship where the initial condition is set to the 1980 real GDP per capita.

Table 8 reports the 2019 country real per capita GDP compared to the counterfactual if there were no learning and state-dependent adaptation for cyclones and heatwaves, respectively. The counterfactual 2019 income for tropical cyclones would be 6.5% lower for the mean or median country income. For heatwaves, the counterfactual 2019 income is around 4% lower.

Panel A of Figure 6 plots the evolution of in-sample and counterfactual country incomes for our cyclone sample. We can see from this figure (and also the summary statistics in Table 8) that the return to adaptation varies across countries — higher for very high and very low income

[17]Strictly speaking, $\hat{\beta}_{i2}$ is estimated using growth rates of GDP net of $(i_{t-1} - \delta)$. However, the growth rates of GDP and GDP per capita are extremely correlated.

Figure 5: Scatter plots of residualized $\hat{\beta}_{2i}$ against $\hat{\lambda}_{B,i} - \hat{\lambda}_{G,i}$

Residualized $\hat{\beta}_{2i}$ on the vertical axis are the country-level second-stage risk-dependent adaptation parameter estimates $\hat{\beta}_{2i}$ residualized in the cross section against $\hat{\pi}_{0,i}$. $\hat{\lambda}_{B,i} - \hat{\lambda}_{G,i}$ on the horizontal axis denotes the country-level $\hat{\lambda}_{B,i} - \hat{\lambda}_{G,i}$ estimates. The red dashed line in each plot is the linear best-fit line, and its estimates are shown in the equation with the $t$-statistic (bootstrapped standard error) for the slope estimate shown in parentheses below the estimate.

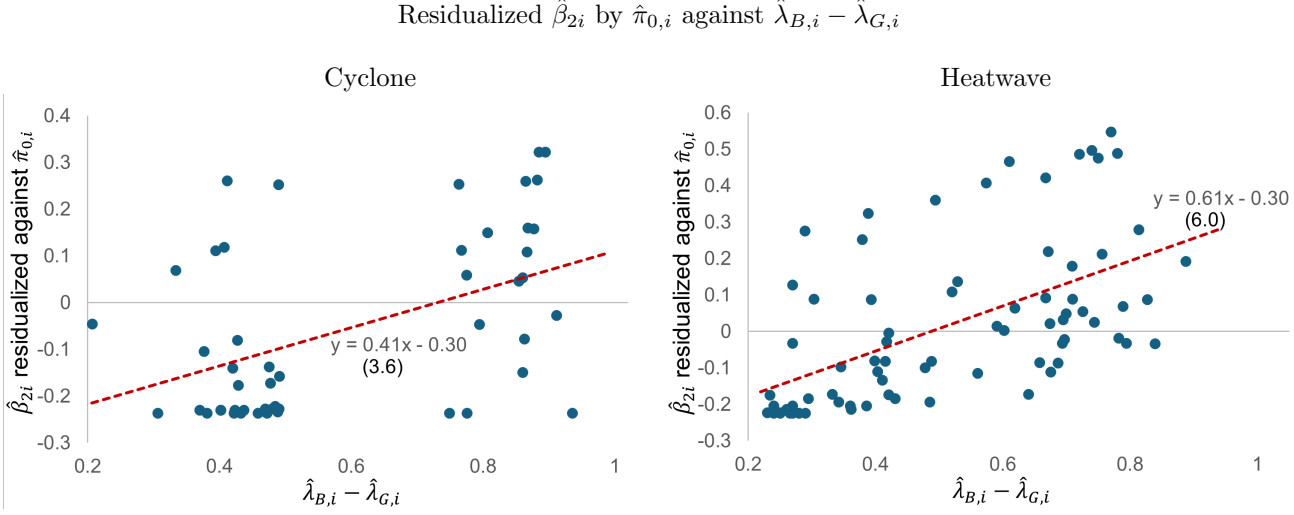


countries. Panel B of Figure 6 plots the evolution of actual and counterfactual incomes absent adaptation for heatwaves. Notice that the countries in the heatwaves sample differ somewhat from the tropical cyclone samples, which is reflected in the larger standard deviation in the heatwave sample.

Table 8: Summary statistics of counterfactual real GDP per capita in 2019

This table presents the summary statistics of the counterfactual real GDP per capita across countries in 2019 by shutting down the risk-dependent adaptation channel and using the in-sample extreme-weather arrival data. Real GDP per capita is in thousands of constant 2015 USD.

| Counterfactual real GDP per capita in 2019 | | | | |
|---|---|---|---|---|
| | Cyclone sample | | Heatwave sample | |
| | In-sample at 2019 | Counterfactual | In-sample at 2019 | Counterfactual |
| Mean | 14.2 | 13.3 | 15.2 | 14.6 |
| S.D. | 19.5 | 19.1 | 21.5 | 21.9 |
| Median | 5.2 | 4.7 | 4.9 | 4.6 |
| P25 | 2.0 | 1.5 | 1.6 | 1.5 |
| P75 | 14.5 | 11.4 | 19.0 | 16.0 |

Figure 6: In-sample counterfactual real GDP per capita absent learning and state-dependent adaptation

This figure shows the in-sample counterfactual (without risk-dependent adaptation) real GDP per capita compared to the actual time-series of real GDP per capita from 1980 to 2019. Panel A shows the results for the cyclone sample and Panel B for the heatwave sample. The left figure in each panel (Actual) shows the actual in-sample time-series paths of real GDP per capita, while the right figure shows the counterfactual income with no learning and state-dependent adaptation. Real GDP per capita is shown in thousands of constant 2015 USD.

**Panel A: Cyclone sample**

Left: Actual. Right: Counterfactual

**Panel B: Heatwave sample**

Left: Actual. Right: Counterfactual

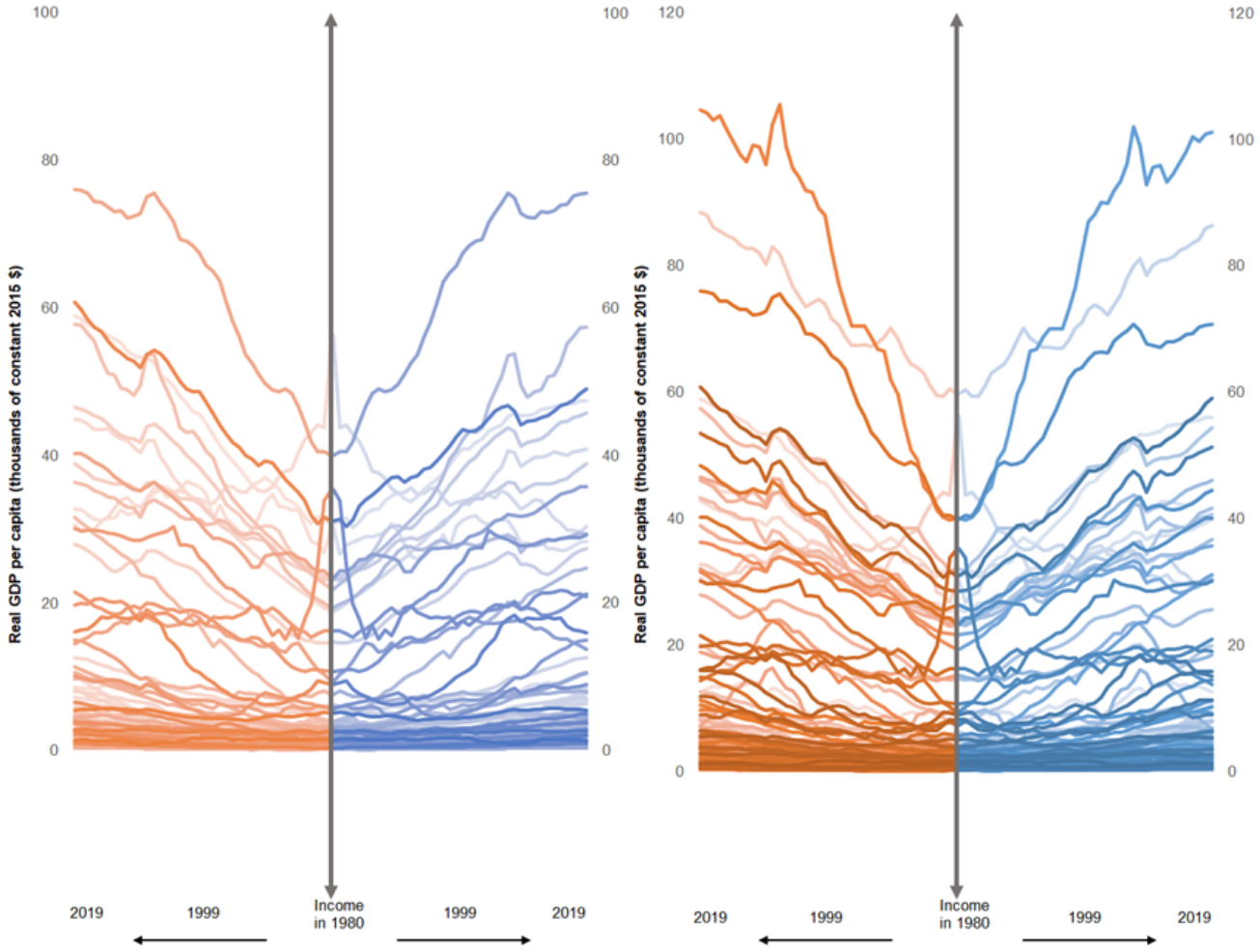

**Evolution of $\hat{\pi}_{it}$ in sample.** To see why income absent adaptation is lower, it is instructive to see how $\hat{\pi}_{it}$ changes over our sample. Figure 7 plots $\hat{\pi}_{it}$ for 1989, 1999, 2009 and 2019.

Consider the heatwave or extreme temperature sample. Here, we see that in 1979 there is little risk of heatwaves as most countries' values of $\hat{\pi}_{it}$ are at around 0.2. However, over the ensuing decades, some of these countries transition to higher $\hat{\pi}_{it}$.[18] The benefit of adaptation is largest for the countries that start from a low $\hat{\pi}_{it}$ in the beginning of the sample and move to a high $\hat{\pi}_{it}$ at the end of the sample. The reason is that these countries are being hit more frequently by disasters and hence lack of adaptation gets penalized more in Equation (10). At the same time, countries that start with a moderate risk and transition to lower $\hat{\pi}_{it}$ over time would be less likely to get hit and hence the adjustment accounting for adaptation matters less for these countries.

A similar logic applies to tropical cyclones. Notice that for cyclones, we see a more dispersed $\hat{\pi}_{i0}$ across countries in 1979 than for heatwaves. For instance, there are some countries with values of $\hat{\pi}_{it}$ above 0.8, but most of the countries are clustered below 0.2. Over time, notice that there are more countries at the extremes of the $\hat{\pi}_{it}$ distribution.[19]

Figure 7: In-sample evolution of $\hat{\pi}_{it}$

This figure plots the in-sample evolution of $\hat{\pi}_{it}$ from 1979 to 2019. The scatter plot of $\hat{\pi}_{it}$ values is shown at each decade end. The darker color the more country observations for those values of $\hat{\pi}_{it}$.

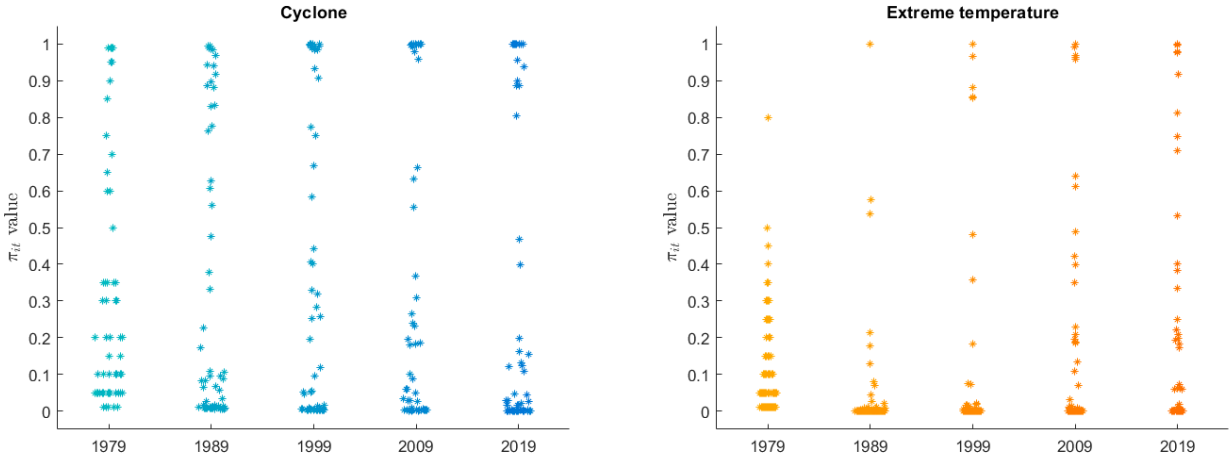


[18]These countries, all with priors between 0.15 and 0.3, include Zambia, Nicaragua, Lebanon, Norway, Mongolia, Spain, The Bahamas, Algeria, Kuwait, Tunisia.

[19]These countries include Honduras, Cambodia, El Salvador, Belize, Fiji, Panama, Dominican Republic, Costa Rica, Guatemala, Nicaragua.

## 8.2 Out of Sample: 2020 to 2050

A fundamental challenge in the literature is to consider how adaptation will affect outcomes in the long run, i.e., standing today, how would income in 2050 differ with adaptation? Taking into account learning and state-dependent adaptation is particularly crucial for this exercise. A country at low prior risk standing in 2019 but which then receives bad realizations and moves to high risk over time has scope to adapt. Hence, ignoring this learning dimension will overstate damages for these countries going forward.

By explicitly modeling the learning or belief process in the first-stage, we are able to not only estimate the returns to adaptation in sample, but to also assess the value of adaptation in the long-run by simulating the evolution of beliefs based on the parameters of the disaster process that we have estimated for each country. Such projections are valuable inputs for calibrating integrated assessment models (Nordhaus (2017), Golosov, Hassler, Krusell, and Tsyvinski (2014)), as is emphasized by Barnett, Brock, and Hansen (2020).

Another way to demonstrate the usefulness of our model is to consider the following common exercise in the climate literature, which is to project the impact of extreme weather events on economic growth over the coming century. We use the estimates from our constant-coefficient model and varying-coefficient model to generate projected future changes in GDP (i.e., growth rates). In particular, the evolution of real GDP per capita in country $i$ in year $t$ is given by:

$$GDP_{it} = GDP_{it-1} \times (1 + \eta_{it} + \chi_{it} D_{it}), \tag{11}$$

where $GDP$ denotes the real GDP per capita. We take 2019 to be $t = 0$. The exercise starts from $t = 1$ and ends in $t = 51$ for year 2050.

In Equation (11), $\eta_{it}$ is the growth rate of $GDP$ of country $i$ in year $t$ absent any climate (extreme weather) damage. As in the literature (e.g., Burke, Hsiang, and Miguel (2015)), we take this base growth rate from the SSP5 (Shared Socio-Economic Pathway, Scenario 5, called "Fossil-Fueled Development" (Kriegler, Bauer, Popp, Humpenöder, Leimbach, Strefler, Baumstark, Bodirsky, Hilaire, Klein, et al. (2017))). $D_{it}$ as before is the dummy variable denoting the extreme weather arrival event for country $i$ in year $t$. The key quantity is $\chi_{it}$, which is the estimated damage of an extreme weather event. We consider two different models for $\chi_{it}$:

a. The damage estimates from the time-invariant regression model. In this case, $\chi_{it}$ is a constant, $\forall(i,t)$, i.e., where adaptation is fixed at prior risk. We call this projection "Fixed Adaptation".

b. The damage estimates from the time-varying model with learning and adaptation, which are shown in Figure 3. In this case, $\chi_{it} = \left(F(\pi_{i0}) + F'(\pi_{i0})\widetilde{\pi}_{it-1}\right)$, which depends on beliefs $\pi_{it-1}$. We call this projection "Risk-dependent Adaptation".

We use the time-varying extreme-weather arrivals model to simulate paths of future extreme weather arrivals. This simulation is rather similar to the one used in our earlier simulated method of moments estimation for beliefs in Section 4. Specifically, for any country $i$ at future year $t$, we simulate the extreme weather arrival at $t$ from the mixed Poisson process: with probability $\pi_{it-1}$ we draw from the high Poisson jump arrival rate $\lambda_{iB}$, and with probability $(1 - \pi_{it-1})$ we draw from the low arrival rate $\lambda_{iG}$. Then we update beliefs $\pi_{it}$ according to the belief-updating equation in Section 4. The simulation runs iteratively from $t = 1$: year 2020 to $t = 51$: year 2050 (remember we have already estimated all the learning parameters $\theta = (\pi_{i0}, \lambda_{iB}, \lambda_{iG})'$ in Section 4 for each country), and we obtain the simulated path of future extreme weather arrivals (as well as future beliefs).

Table 9: Summary statistics of projected real GDP per capita in 2050, mixture model

This table presents the summary statistics of projected real GDP per capita across countries in 2050 using SSP5 and simulated arrivals from the time-varying extreme-weather arrivals model (Section 4) for both the cyclone and the heatwave sample. Real GDP per capita is in thousands of constant 2015 USD. We consider two scenarios: adaptation fixed at prior risk and risk-dependent adaptation.

| Projected real GDP per capita in 2050, mixture model simulation | | | | |
|---|---|---|---|---|
| | Cyclone sample | | Heatwave sample | |
| | Fixed | Risk-dependent | Fixed | Risk-dependent |
| Mean | 27.6 | 31.8 | 26.0 | 30.9 |
| S.D. | 23.0 | 26.6 | 24.0 | 29.5 |
| Median | 18.4 | 21.2 | 15.5 | 17.9 |
| P5 | 4.8 | 6.3 | 3.8 | 4.8 |
| P25 | 12.2 | 13.9 | 9.0 | 10.2 |
| P75 | 38.4 | 40.7 | 35.1 | 41.4 |
| P95 | 73.4 | 82.3 | 73.9 | 86.8 |

In Table 9, we report the projections for GDP in 2050, both for the cyclone sample and the extreme temperature sample. For the tropical cyclones sample, there is a significant difference in projected income depending on whether one accounts for learning and risk-dependent adaptation. Using the constant-coefficient model that does not account for heterogeneity in risk-dependent adaptation across countries, the mean income is 27.6 thousand dollars. Adding learning and risk-dependent adaptation increases income from 27.6 thousand to 31.8 thousand dollars. That is, income with fixed adaptation would be nearly 13% lower than with risk-dependent adaptation. For extreme temperature, income with fixed adaptation would be nearly

15% lower than with risk-dependent adaptation. In other words, ignoring learning considerably overstates the damage from extreme-weather risks over long horizons.

Figure 8: Projections of real GDP per capita, mixture model, 2020 to 2050

This figure shows projections of real GDP per capita using simulated arrivals from the time-varying extreme-weather arrivals model. Panel A shows the results for the cyclone sample and Panel B for the heatwave sample. The left figure in each panel (Risk-dependent Adaptation) uses adaptation estimates from the varying coefficient model and belief updates according to the simulated arrivals, while the right figure (Fixed Adaptation) uses damage estimates from the constant coefficient model. Real GDP per capita is shown in thousands of constant 2015 USD. Projections are shown from 2019 to 2050. We run 10,000 simulations for each country and take the median of the simulations as its projection. The baseline GDP growth projections without extreme weather damages come from the SSP5 (Shared Socio-Economic Pathway, Scenario 5, called "Fossil-Fueled Development" — Kriegler, Bauer, Popp, Humpenöder, Leimbach, Strefler, Baumstark, Bodirsky, Hilaire, Klein, et al. (2017)).

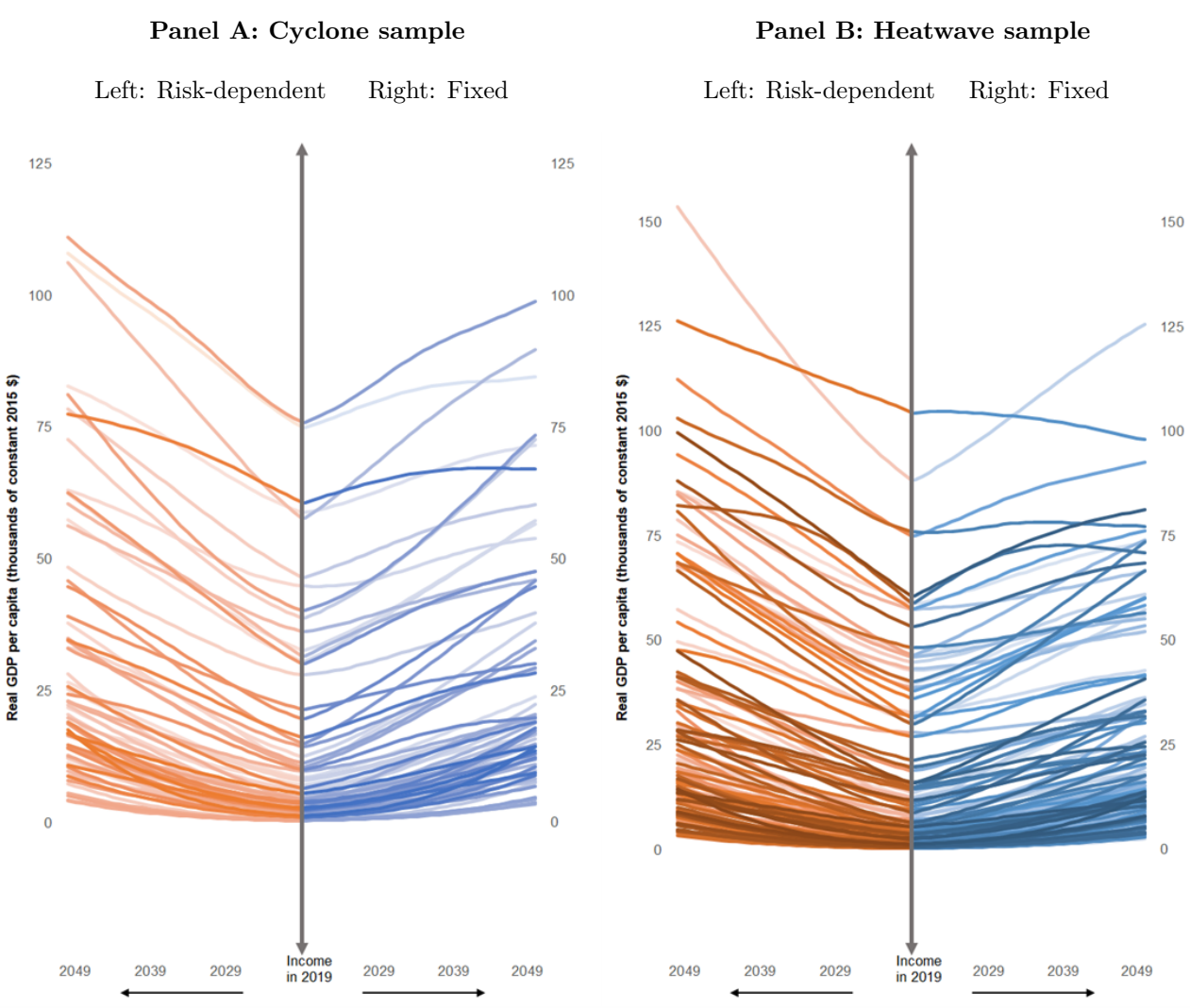


To see these differences country by country, in Figure 8, we report the projections for GDP

using simulations of the time-varying arrivals model of Section 4. In Panel A, for the tropical cyclones sample, there is a significant difference depending on whether we account for learning (left side of the graphs) versus not doing so (right side of the graphs). The same is true for the extreme temperature sample in Panel B.[20]

**Resolution of uncertainty in long run.** To understand why adjusting for learning is more important for sample projections than in-sample counterfactuals, we plot in Figure 9 the evolution of $\pi_{it}$ for all countries from the end of our sample in 2019 to near the end of projection period in 2049. We show the scatter plot of $\pi_{it}$ values.

Let us compare the cyclone-risk evolution out of sample in Figure 9 to the analogous in-sample Figure 7. We can see considerably more dispersion in outcomes across countries in 2049. The same is true for the extreme temperature sample. This dispersion driven by uncertainty resolution means that adaptation becomes more valuable over the long run.

Figure 9: Evolution of $\pi_{it}$ over time

This figure plots the evolution of $\pi_{it}$ over time at every 5 years from the sample end to the projection end. The scatter plot of $\pi_{it}$ values is shown at each 5-year end.


# 9 Alternative Time-Varying Risk Models

In this section, we show that our empirical findings are robust to using deterministic time-trend models for the arrival of disaster, which differ from our baseline model in terms of martingale

[20] In Table O.5, we show that the results from a second-order Taylor approximation of the non-linear damage function are the same as those from a first-order Taylor approximation.

properties but nonetheless generate correlated forecasts.

## 9.1 Time-Trend Models

Another way to model the time in-homogeneity of disaster arrivals is by letting the intensity function vary over time. If $N_t : t \geq 0$ is the counting process that records the number of events up to time $t$, a deterministic time trend model is defined through an intensity function $\lambda_t$ such that the expected increment in $N_t$ over an infinitesimal interval $(t, t + dt]$ is $\lambda_t dt$ and the increments are independent.

The intensity function is typically parameterized to ensure positivity through a log-linear model:

$$\lambda_t = \exp(x_t'\theta), \tag{12}$$

where $x_t$ is a vector of covariates (possibly including deterministic functions of time) and $\theta$ is the parameter vector to be estimated. We consider two models for $\lambda_t$, both of which are deterministic functions of time:

$$\lambda_t = \exp(\theta_0 + \theta_1 t) \quad \text{the trend model (linear time trend)}, \tag{13}$$

$$\lambda_t = \exp(\theta_0 + \theta_1 t + \theta_2 t^2) \quad \text{the quadratic } t \text{ model (quadratic time trend)}. \tag{14}$$

In Appendix B.1, we present the log-likelihood function and how to obtain estimates of the $\theta_i$'s. We can also reject the null i.i.d. Poisson model using the linear and quadratic time trend models. Rather than repeat these obvious results, we instead in Appendix B.2 conduct a Vuong (1989) non-nested specification test of our mixture model against the linear time trend model in Table B.1.

For cyclones, the mixture model is preferred to the linear time trend model for 83% of the countries. For heatwaves, the mixture model is preferred in 51%; for 27% of the countries, the two models are indistinguishable. The results are expected as the frequency of cyclones have exhibited little time trends (Knutson, Camargo, Chan, Emanuel, Ho, Kossin, Mohapatra, Satoh, Sugi, Walsh, et al. (2020)), while heatwaves in a number of regions have prominent time trends (Perkins-Kirkpatrick and Lewis (2020)).

In Table B.2, we compare the mixture model to the quadratic time trend model. For cyclones, the mixture model is preferred in 37% of the countries versus 31% for the quadratic time-trend model. For heatwaves, the analogous figures are 44% to 28%. These findings suggest that the mixture model provides a good fit of the data on disaster arrivals.

### 9.2 Return to Adaptation with Time-Trend Models

In Appendix B.3, we compare the second-stage estimates obtained from a first-stage risk dynamics using our mixture model to second-stage estimates obtained from using the deterministic linear and quadratic time-trend models. Regardless of the model, the distribution for $\hat{\beta}_{2i}$ has a statistically significant non-zero mean. In other words, our conclusions regarding risk-dependent adaptation are robust to the first-stage risk dynamics as long as the dynamics provides an adequate fit of the data.

### 9.3 Counterfactuals with Time-Trend Models

Finally, our conclusions regarding counterfactuals are similar if we use the deterministic time-trend models. For instance, in Appendix B.4, we show that our conclusions hold also with projections using the deterministic time trend models. Over long horizons, forecasts from both approaches are correlated, but the mixture model with Bayesian updating provides the structural interpretation of risk as a martingale, whereas trend-based models can be viewed as sub- or super-martingales.

## 10 Conclusion

This paper develops a new empirical framework to measure the economic return to adaptation in a changing climate. The approach combines a statistical model of disaster risk with an economic model of state-dependent damages. This parsimonious structure accounts for the volatility clustering observed in disaster data and provides a tractable basis for estimating how adaptation varies with perceived risk. Across global panels of tropical cyclones and extreme temperatures, we find that economic damages are systematically lower when disaster risk is high. This pattern is consistent with risk-based adaptation. The implied return to adaptation is larger for countries where disaster arrivals are more non-i.i.d., that is, where exposure to high-risk regimes is more frequent or predictable. Our results indicate that adaptation yields substantial long-run economic returns as uncertainty about climate risk resolves. Importantly, our findings are robust across underlying perceived-risk processes with distinct martingale properties.

# References


Auffhammer, M. (2022): "Climate adaptive response estimation: Short and long run impacts of climate change on residential electricity and natural gas consumption," Journal of Environmental Economics and Management, 114, 102669.

Bakkensen, L. A., and R. O. Mendelsohn (2016): "Risk and Adaptation: Evidence from Global Hurricane Damages and Fatalities," Journal of the Association of Environmental and Resource Economists, 3(3), 555–587.

Baltagi, B. (2008): "To Pool or Not to Pool," in The Econometrics of Panel Data, vol. 46, pp. 517–546.

Barnett, M., W. Brock, and L. P. Hansen (2020): "Pricing uncertainty induced by climate change," The Review of Financial Studies, 33(3), 1024–1066.

Barreca, A., K. Clay, O. Deschenes, M. Greenstone, and J. S. Shapiro (2016): "Adapting to Climate Change: The Remarkable Decline in the US Temperature-Mortality Relationship over the Twentieth Century," Journal of Political Economy, 124(1), 105–159.

Bilal, A., and D. R. Känzig (2024): "The macroeconomic impact of climate change: Global vs. local temperature," Discussion paper, National Bureau of Economic Research.

Bouwer, L. M., R. P. Crompton, E. Faust, P. Höppe, and R. A. Pielke Jr (2007): "Confronting disaster losses," Science, 318(5851), 753–753.

Burke, M., S. M. Hsiang, and E. Miguel (2015): "Global non-linear effect of temperature on economic production," Nature, 527(7577), 235–239.

Carleton, T., A. Jina, M. Delgado, M. Greenstone, T. Houser, S. Hsiang, A. Hultgren, R. E. Kopp, K. E. McCusker, I. Nath, J. Rising, A. Rode, H. K. Seo, A. Viaene, J. Yuan, and A. T. Zhang (2022): "Valuing the Global Mortality Consequences of Climate Change Accounting for Adaptation Costs and Benefits," The Quarterly Journal of Economics, 137(4), 2037–2105.

Chen, X., H. Hong, and M. Shum (2007): "Nonparametric likelihood ratio model selection tests between parametric likelihood and moment condition models," Journal of Econometrics, 141(1), 109–140.

Daley, D. J., and D. Vere-Jones (2003): "An Introduction to the Theory of Point Processes: Volume I: Elementary Theory and Methods," Springer.

Dell, M., B. F. Jones, and B. A. Olken (2012): "Temperature shocks and economic growth: Evidence from the last half century," American Economic Journal: Macroeconomics, 4(3), 66–95.

Dell, M., B. F. Jones, and B. A. Olken (2014): "What Do We Learn from the Weather? The New Climate-Economy Literature," Journal of Economic Literature, 52(3), 740–98.

Deschênes, O., and M. Greenstone (2007): "The economic impacts of climate change: Evidence from agricultural output and random fluctuations in weather," American Economic Review, 97(1), 354–385.

Duffie, D., and K. J. Singleton (1993): "Simulated moments estimation of Markov models of asset prices," Econometrica, 61, 929–952.

Golosov, M., J. Hassler, P. Krusell, and A. Tsyvinski (2014): "Optimal taxes on fossil fuel in general equilibrium," Econometrica, 82(1), 41–88.

Gourio, F., and C. Fries (2020): "Adaptation and the Cost of Rising Temperature for the U.S. Economy," Working paper, Federal Reserve Bank of Chicago.

Greene, W. H. (2012): "Econometric Analysis, 7th Edition," Prentice Hall.

Hong, H., N. Wang, and J. Yang (2023): "Mitigating Disaster Risks in the Age of Climate Change," Econometrica, 91(5), 1763–1802.

Hsiang, S. M., and A. S. Jina (2014): "The Causal Effect of Environmental Catastrophe on Long-Run Economic Growth: Evidence From 6,700 Cyclones," Working paper, National Bureau of Economic Research.

Knutson, T., S. J. Camargo, J. C. Chan, K. Emanuel, C.-H. Ho, J. Kossin, M. Mohapatra, M. Satoh, M. Sugi, K. Walsh, et al. (2020): "Tropical cyclones and climate change assessment: Part II: Projected response to anthropogenic warming," Bulletin of the American Meteorological Society, 101(3), E303–E322.

Kriegler, E., N. Bauer, A. Popp, F. Humpenöder, M. Leimbach, J. Strefler, L. Baumstark, B. L. Bodirsky, J. Hilaire, D. Klein, et al. (2017): "Fossil-fueled development (SSP5): An energy and resource intensive scenario for the 21st century," Global Environmental Change, 42, 297–315.

Kutoyants, Y. A. (1998): "Statistical Inference for Spatial Poisson Processes," Springer-Verlag.

Lipster, R. S., and A. Shiryaev (2001): Statistics of Random Processes II: Applications. Springer-Verlag, New York.

National Academies of Sciences, Engineering, and Medicine (2016): Attribution of extreme weather events in the context of climate change. National Academies Press.

Nordhaus, W. D. (2017): "Revisiting the social cost of carbon," Proceedings of the National Academy of Sciences, 114(7), 1518–1523.

Perkins-Kirkpatrick, S., and S. Lewis (2020): "Increasing trends in regional heatwaves," Nature Communications, 11(1), 3357.

Pesaran, M. H., and R. Smith (1995): "Estimating Long-Run Relationships from Dynamic Heterogeneous Panels," Journal of Econometrics, 68, 79–113.

Pindyck, R. S., and N. Wang (2013): "The economic and policy consequences of catastrophes," American Economic Journal: Economic Policy, 5(4), 306–339.

Rivers, D., and Q. H. Vuong (2002): "Model selection tests for nonlinear dynamic models," Econometrics Journal, 5, 1–39.

Schlenker, W., and M. J. Roberts (2009): "Nonlinear temperature effects indicate severe damages to US crop yields under climate change," Proceedings of the National Academy of sciences, 106(37), 15594–15598.

Sisco, M. R., V. Bosetti, and E. U. Weber (2017): "When do extreme weather events generate attention to climate change?," Climatic Change, 143, 227–241.

Vuong, Q. H. (1989): "Likelihood ratio tests for model selection and non-nested hypotheses," Econometrica, 57(2), 307–333.

Willmott, C. J., and K. Matsuura (2018): "Terrestrial air temperature: 1900-2008 gridded monthly time series," Center for Climatic Research, University of Delaware, Newark. http://climate.geog.udel.edu/climate.

# Appendix

# A Model Diagnostics

## A.1 Linear vs Nonlinear Damage Function

We can check the adequacy of the linear model (7) used in the second stage. Let $\hat{\varepsilon}_t$ be the residuals from estimation of (7) for a given country. Theory suggests that economic outcomes should depend not only on $D_t$, but also on $\pi_t$ in a possibly non-linear way. Consider the regression

$$\hat{\varepsilon}_t = \gamma_0 + \gamma_1 D_t + \gamma_2 D_t \pi_{t-1} + \gamma_3 \pi_{t-1} + \text{err}_t. \tag{A.1}$$

Under the null hypothesis that the linear model is correct, $\pi_t$ and the interaction term should have no explanatory power and the $R^2$ of the above regression should be small. The LM test statistic $T \cdot R^2$ has a $\chi^2$ distribution with two degrees of freedom. As shown below, the results resoundingly reject the null hypothesis. On average, the $R^2$ in these regressions is over 0.18, indicating non-trivial explanatory power in the omitted terms. Table A.1 shows the percentage of countries for which the LM test rejects the null hypothesis of the linear model being correctly specified. We can see that for most of countries, the LM test rejects at the usual statistical significance levels. This result suggests that omitted non-linear terms from the linear model can explain nearly 20% of the variations in the residuals.

Table A.1: Specification Tests: % of countries rejecting null hypothesis $H_0$ at 10 and 5% significance levels

This table presents the results of our model diagnostics. The first row shows the summary statistics over all countries of country-level LM tests for the adequacy of the linear damage function model against the alternative adaptation model with additional $D_t\pi_{t-1}$ and $\pi_{t-1}$ terms. The second row shows the summary statistics of country-level Breusch–Godfrey tests for 1st-order residual serial correlations in the adaptation regression.

| Model | Equation | $H_0$ | Cyclone | | Heatwave | |
|---|---|---|---|---|---|---|
| | | | 10% | 5% | 10% | 5% |
| Residual of linear model | (A.1) | $\gamma_1 = \gamma_2 = \gamma_3 = 0$ | 91.3 | 72.5 | 92.6 | 71.2 |
| Residual of nonlinear model | (8) | Breusch-Godfrey | 2.2 | 0 | 4.1 | 0 |

## A.2 Residual Serial Correlation Test of Nonlinear Model

To further confirm the adequacy of our model with learning and adaptation, we conduct tests for first-order residual serial correlations of our nonlinear model in Section 4.2 with the estimates

given in Section 6. We find no evidence of serial correlation in Table A.1. For the 10% level of significance, we find that only in 3% of countries can we reject the null hypothesis of no serial correlation in the residuals for cyclones. For the 5% level of significance, it is 0%. For the extreme temperature model, only in 4% of the countries can we reject the null at the 10% level and 0% at the 5% level of significance.[21]

## A.3 Global Detrending

For our key estimation equation (8), we detrend the variables as follows. For any variable $w_{it}$ where $i$ indexes country and $t$ indexes time, define $\bar{w}_{i\cdot} = (1/T)\sum_{t=1}^{T} w_{it}$, $\bar{w}_{\cdot t} = (1/N)\sum_{i=1}^{N} w_{it}$, $\bar{w} = (1/N)(1/T)\sum_{i=1}^{N}\sum_{t=1}^{T} w_{it}$, and the detrended version of $w_{it}$ is $\ddot{w}_{it} = w_{it} - \bar{w}_{i\cdot} - \bar{w}_{\cdot t} + \bar{w}$. Then we estimate the following detrended version of our main equation (8) country by country

$$\ddot{y}_{it} = \alpha_i + \beta_{1i}\ddot{D}_{it} + \beta_{2i}\ddot{x}_{it} + \epsilon_{it}$$

where $y_{it} = g_{it} - (i_{it-1} - \delta_{it-1})$, $x_{it} = \tilde{\pi}_{it-1}D_{it}$, and $\alpha_i$ is statistically equal to zero. This detrending is equivalent to removing the country and time effects from a pooled panel regression model.[22] We show the detrended results in Figure O.1. The estimates of $\beta_{1i}$ and $\beta_{2i}$ are quite close to our baseline model estimates in Figure 3. Hence detrending has no impact on our main findings.

## A.4 Panel Regression Estimates of the Risk-Dependent Model

We estimate our risk-dependent model in a pooled panel regression with country and year fixed effects as another robustness check. The estimates, which are similar to those that we obtain by averaging our country-by-country estimates, are shown in Table O.4.

[21] Because the residuals from our nonlinear model are serially uncorrelated, it does not matter if we also control for lagged GDP growth and the interaction of lagged GDP growth with the disaster arrival indicator $D_{it}$ in our empirical analysis.

[22] See Greene (2012), chapter 11.4 for reference.

# B Deterministic Time-Trend Models of Disaster Arrivals

## B.1 Estimation

For our observations of 0/1 arrival indicators $D_t; t = 1, \ldots, T$, the likelihood function of the time-trend model is (see Daley and Vere-Jones (2003) and Kutoyants (1998) for a reference):

$$L(\theta) = \exp\Big( -\sum_{t=1}^{T} \lambda_t \Big) \prod_{t=1}^{T} \lambda_t^{D_t}, \tag{B.1}$$

where $\lambda_t$ is either the trend model specified in (13) or the quadratic model specified in (14). The log-likelihood function is therefore:[23]

$$\mathcal{L}(\theta) = -\sum_{t=1}^{T} \lambda_t + \sum_{t=1}^{T} D_t \log\big(\lambda_t\big). \tag{B.2}$$

The parameter vector $\theta$ of our time-trend models can then be directly estimated by maximum likelihood using the log-likelihood function (B.2).

Once we obtain the estimated parameter vector $\hat{\theta}$ of our time-trend models, we can then calculate the estimated $\hat{\lambda}_t^{trend}$ of the model, where $\hat{\lambda}_t^{trend} = \exp(\hat{\theta}_0 + \hat{\theta}_1 t)$ for the trend model and $\hat{\lambda}_t^{trend} = \exp(\hat{\theta}_0 + \hat{\theta}_1 t + \hat{\theta}_2 t)$ for the quadratic model. We do this country by country, so we have suppressed the country subscript $i$ from the notations for notation ease.

**Obtaining $\hat{\lambda}_t$ from our mixture model.** From our baseline mixture model, we can directly obtain the estimated $\hat{\lambda}_t^{\pi}$ using the estimates of $\{\hat{\lambda}_B, \hat{\lambda}_G, \hat{\pi}_t\}$: $\hat{\lambda}_t^{\pi} = \hat{\pi}_t \hat{\lambda}_B + (1 - \hat{\pi}_t)\hat{\lambda}_G$. We do this country by country, so we have suppressed the country subscript $i$ from the notations for notation ease.

## B.2 Non-Nested Model Specification Test

We conduct the Vuong (1989) non-nested model specification test (see also Chen, Hong, and Shum (2007)) for the mixture model v.s. one of the deterministic time-trend models.

The test can be conducted by calculating the values of the log-likelihood from each model based on the model's parameter estimates.

[23] See Equation (7.1.2), Chapter 7.1 of Daley and Vere-Jones (2003) for the same log-likelihood function.

For a time-trend model, the value of the log-likelihood at $t$ is simply

$$\hat{ll}_t^{NHPP} = -\hat{\lambda}_t^{NHPP} + D_t \log\left(\hat{\lambda}_t^{NHPP}\right). \tag{B.3}$$

For the mixture model, we estimated it using SMM since we cannot write down its full-information likelihood function in closed form due to the presence of the stochastic time-varying risks $\pi_t$. However, after we obtain the SMM model parameter estimates, we also have the estimates of $\pi_t$, $\hat{\pi}_t$, constructed from the model parameter estimates and data on the history of arrivals. Then, we can construct an estimated log-likelihood for the mixture model based on the probability density function of a two-state mixed Poisson process with states $\{\hat{\lambda}_B, \hat{\lambda}_G\}$ and mixture probabilities (which vary over $t$) $\{\hat{\pi}_t, (1-\hat{\pi}_t)\}$:

$$\hat{ll}_t^{\pi} = \log\left(\hat{\pi}_t \frac{\exp(-\hat{\lambda}_B)\hat{\lambda}_B^{D_t}}{D_t!} + (1-\hat{\pi}_t)\frac{\exp(-\hat{\lambda}_G)\hat{\lambda}_G^{D_t}}{D_t!}\right). \tag{B.4}$$

Thus we have the estimated value of the log-likelihood at any $t$ for both the mixture model and the time-trend models.

The test statistic of the Vuong (1989) model specification test for the mixture model v.s. one of the time-trend models is

$$V = \sqrt{T}\bar{v}/\hat{\sigma}_v \tag{B.5}$$

where $\bar{v} = (1/T)\sum_{t=1}^{T} v_t$, $\hat{\sigma}_v = (1/T)\sum_{t=1}^{T}(v_t - \bar{v})^2$, and $v_t = \left(\hat{ll}_t^{\pi} - \hat{ll}_t^{trend}\right)$ from above. The test statistic $V$ is asymptotically standard normal, so that at the 5% significance level, if $V > 1.96$, our mixture model is preferred; if $V < -1.96$, the time-trend model is preferred; otherwise the two models are not distinguishable (the test is indeterminate). This test essentially applies the extended Vuong (1989) test (see Rivers and Vuong (2002)) where our selection criterion is based on Kullback-Leibler information criterion (i.e., estimated likelihood values) even though we did not estimate the mixture model by the method of maximum-likelihood but by SMM instead (see also Chen, Hong, and Shum (2007) for a reference).[24]

[24] In Rivers and Vuong (2002), the test allows for the situation where the methods used to estimate the competing models need not optimize the selection criteria used for model selection. This is exactly our case where the method to estimate the mixture model is SMM but the model selection criterion is based on likelihoods.

Table B.1: Vuong (1989) non-nested model specification test for mixture model v.s. linear time trend model

Mixture model is our baseline first-stage model from Section 4. Trend model is the deterministic linear time trend $\lambda_t$ model from Equation (13) in Section 9.1.

| Vuong (1989) test for mixture model v.s. trend model, 5% sig. lvl (non-nested model specification test) | | | |
|---|---|---|---|
| | Cyclone | | |
| | Mixture model preferred | Trend model preferred | Not distinguishable |
| % of all sample countries | 83% | 0% | 17% |
| | Heatwave | | |
| | Mixture model preferred | Trend model preferred | Not distinguishable |
| % of all sample countries | 51% | 22% | 27% |

Table B.2: Vuong (1989) non-nested model specification test for mixture model v.s. quadratic $t$ model

Mixture model is our baseline first-stage model from Section 4. Quadratic $t$ model is the deterministic quadratic time trend $\lambda_t$ model from Equation (14) in Section 9.1.

| Vuong (1989) test for mixture model v.s. quadratic $t$ model, 5% sig. lvl (non-nested model specification test) | | | |
|---|---|---|---|
| | Cyclone | | |
| | Mixture model preferred | Quadratic $t$ model preferred | Not distinguishable |
| % of all sample countries | 37% | 31% | 32% |
| | Heatwave | | |
| | Mixture model preferred | Quadratic $t$ model preferred | Not distinguishable |
| % of all sample countries | 44% | 28% | 28% |

## B.3 Comparing Second-Stage Estimates of Mixture Model to Time-Trend Model

**Second-stage estimation using $\hat{\lambda}_t$.** For the second-stage estimation of $\beta_{1i}$ and $\beta_{2i}$ for both our mixture and time-trend models, we run the following country-by-country regression parameterized in terms of $\hat{\lambda}_{it}$:

$$g_{it}^{n} = \mu_i + \beta_{1i} D_{it} + \beta_{2i} \tilde{\lambda}_{i,t-1} D_{it} + \varepsilon_{it}, \tag{B.6}$$

where $\tilde{\lambda}_{i,t-1} = (\hat{\lambda}_{i,t-1} - \hat{\lambda}_{0,i})$, $\hat{\lambda}_{it}$ is either $\hat{\lambda}_{it}^{\pi}$ (the mixture model) or $\hat{\lambda}_{it}^{NHPP}$ (the time-trend model), and $\hat{\lambda}_{0,i}^{\pi} = \hat{\pi}_{0,i}\hat{\lambda}_{B,i} + (1 - \hat{\pi}_{0,i})\hat{\lambda}_{G,i}$; $\hat{\lambda}_{0,i}^{NHPP} = \exp(\hat{\theta}_{0,i})$.

Hence we obtain two sets of country-level estimates of $\beta_{1i}$ and $\beta_{2i}$, one for the mixture model and the other the time-trend model:

$$(\hat{\beta}_{1i}^{\pi}, \hat{\beta}_{2i}^{\pi}) \; ; \; (\hat{\beta}_{1i}^{NHPP}, \hat{\beta}_{2i}^{NHPP}), \tag{B.7}$$

for which we then plot their densities. In Figures B.1 and B.2, we compare the second-stage estimates from the mixture model of risk to those from the deterministic trend models.

## B.4 Projections Using Quadratic Deterministic Time-Trend Model

In Table B.4, we present the counterfactual income in 2050 using the deterministic quadratic time trend model.

Table B.3: Summary statistics of projected real GDP per capita in 2050, quadratic $t$ model

This table presents the summary statistics of projected real GDP per capita across countries in 2050 using SSP5 and simulated arrivals from the time-varying extreme-weather arrivals of the deterministic quadratic time trend $\lambda_t$ model (quadratic $t$ model, Equation (14) in Section 9.1) for both the cyclone and the heatwave sample. Real GDP per capita is in thousands of constant 2015 USD. We consider two scenarios: adaptation fixed at prior risk and risk-dependent adaptation.

| Projected real GDP per capita in 2050, quadratic $t$ model simulation | | | | |
|---|---|---|---|---|
| | Cyclone sample | | Heatwave sample | |
| | Fixed | Risk-dependent | Fixed | Risk-dependent |
| Mean | 28.0 | 30.9 | 27.7 | 30.5 |
| S.D. | 23.7 | 25.5 | 25.6 | 29.3 |
| Median | 18.6 | 20.5 | 16.3 | 17.7 |
| P5 | 5.1 | 6.1 | 4.2 | 4.7 |
| P25 | 12.4 | 13.3 | 9.5 | 10.0 |
| P75 | 34.5 | 36.2 | 36.2 | 41.1 |
| P95 | 75.9 | 81.9 | 77.6 | 86.5 |

Figure B.1: Density of $\hat{\beta}_{1i}$ and $\hat{\beta}_{2i}$, mixture model v.s. linear time trend model

Mixture model is our baseline first-stage model from Section 4. Trend model is the deterministic linear time trend $\lambda_t$ model from Equation (13) in Section 9.1.

Panel A: Density plot of $\hat{\beta}_{1i}$

Cyclone $\hat{\beta}_{1i}$

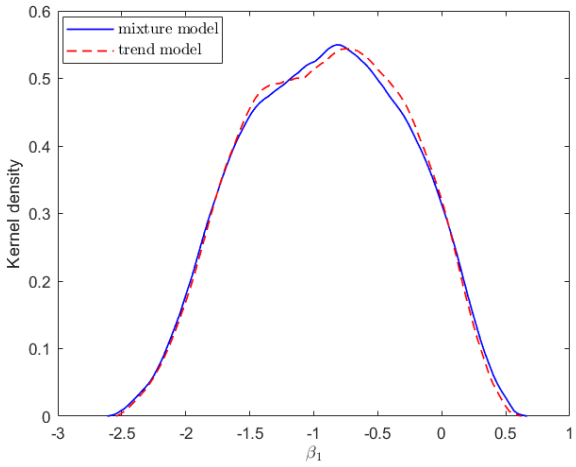


Heatwave $\hat{\beta}_{1i}$

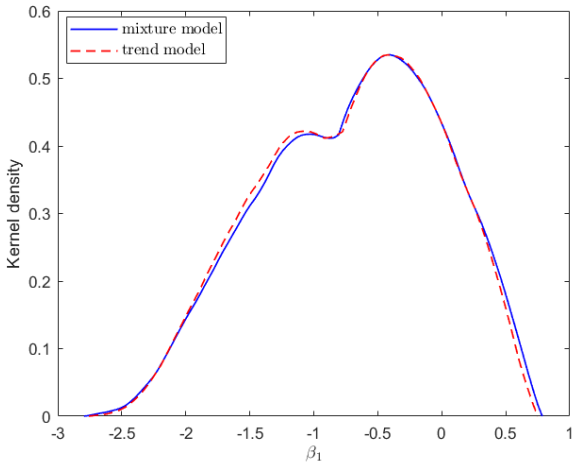


Panel B: Density plot of $\hat{\beta}_{2i}$

Cyclone $\hat{\beta}_{2i}$

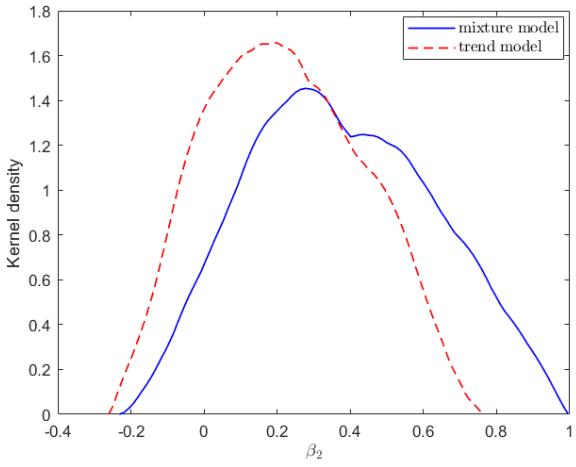


Heatwave $\hat{\beta}_{2i}$

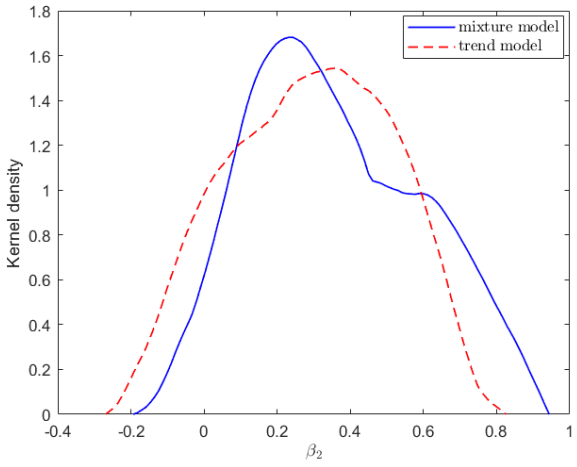

Figure B.2: Density of $\hat{\beta}_{1i}$ and $\hat{\beta}_{2i}$, mixture model v.s. quadratic $t$ model

Mixture model is our baseline first-stage model from Section 4. Quadratic $t$ model is the deterministic quadratic time trend $\lambda_t$ model from Equation (14) in Section 9.1.

Panel A: Density plot of $\hat{\beta}_{1i}$

Cyclone $\hat{\beta}_{1i}$

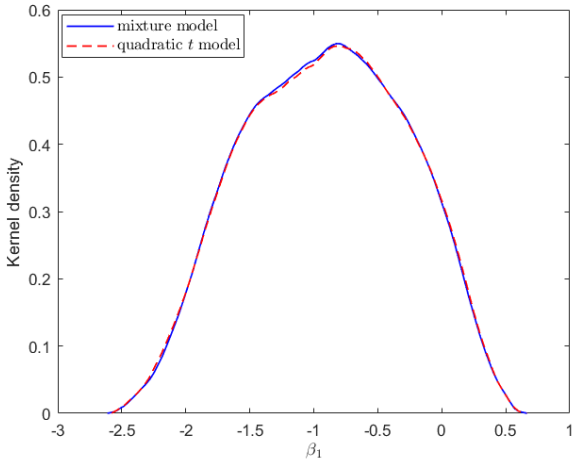


Heatwave $\hat{\beta}_{1i}$

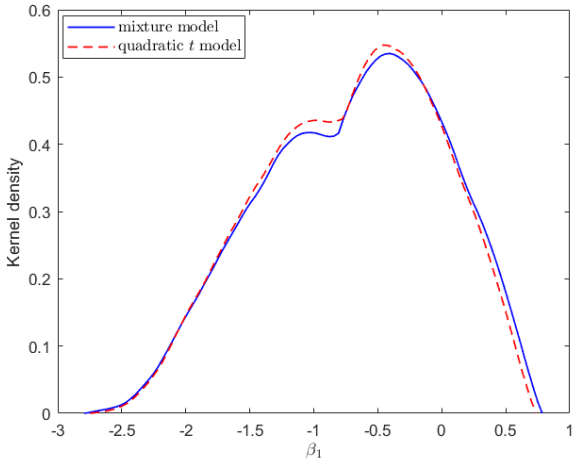


Panel B: Density plot of $\hat{\beta}_{2i}$

Cyclone $\hat{\beta}_{2i}$

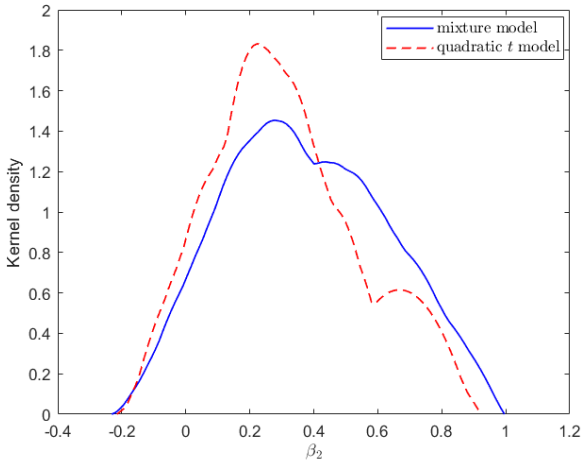


Heatwave $\hat{\beta}_{2i}$

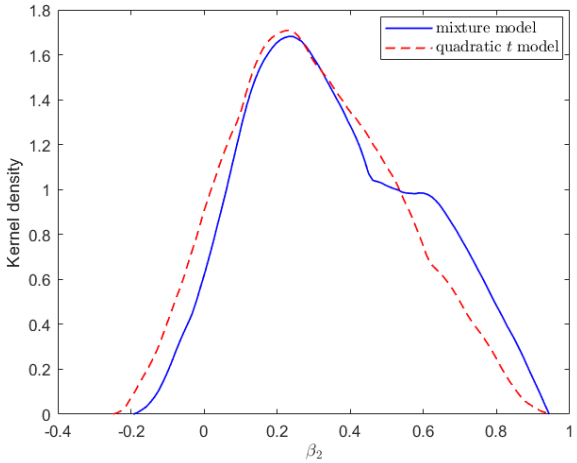

Figure B.3: Projections of real GDP per capita, quadratic $t$ model, 2020 to 2050

This figure shows projections of real GDP per capita using simulated arrivals from the deterministic quadratic time trend $\lambda_t$ model (quadratic $t$ model, Equation (14) in Section 9.1). Panel A shows the results for the cyclone sample and Panel B for the heatwave sample. The left figure in each panel (Risk-dependent Adaptation) uses adaptation estimates from the varying coefficient model and belief updates according to the simulated arrivals, while the right figure (Fixed Adaptation) uses damage estimates from the constant coefficient model. Real GDP per capita is shown in thousands of constant 2015 USD. Projections are shown from 2019 to 2050. We run 10,000 simulations for each country and take the median of the simulations as its projection. The baseline GDP growth projections without extreme weather damages come from the SSP5 (Shared Socio-Economic Pathway, Scenario 5, called "Fossil-Fueled Development" — Kriegler, Bauer, Popp, Humpenöder, Leimbach, Strefler, Baumstark, Bodirsky, Hilaire, Klein, et al. (2017)).

**Panel A: Cyclone sample**

Left: Risk-dependent Right: Fixed

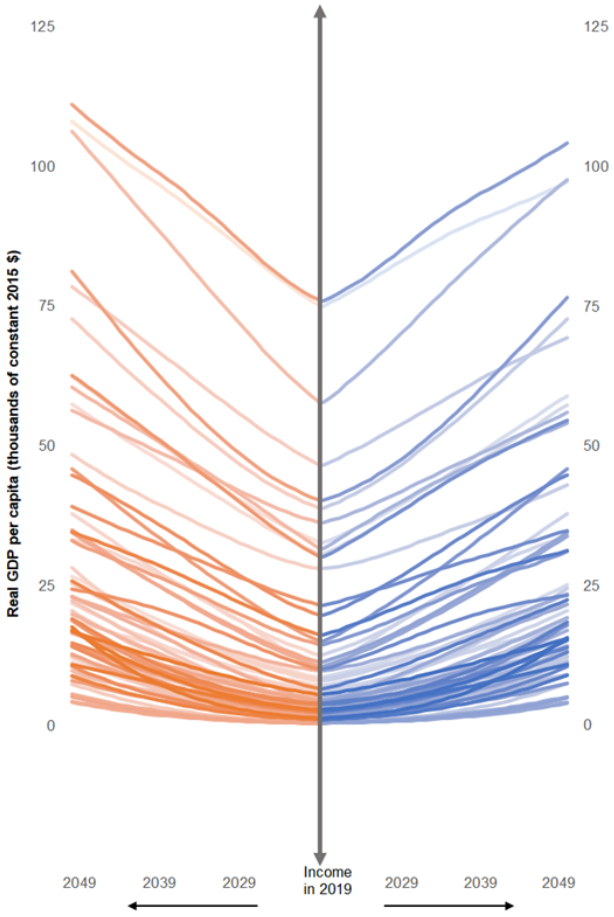


**Panel B: Heatwave sample**

Left: Risk-dependent Right: Fixed

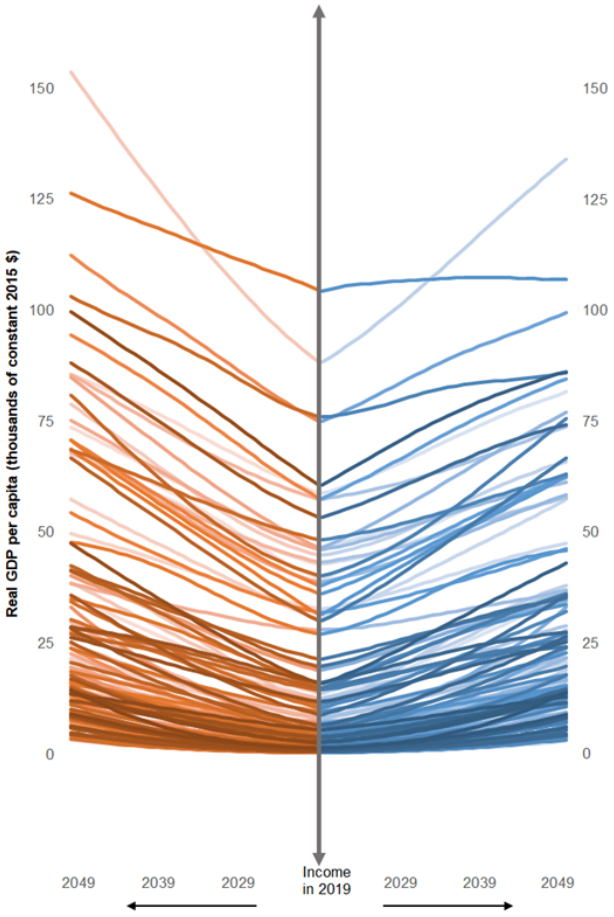

# Supplementary Appendix for Online Publication Only

The following supplementary tables and figures are for Hong, Ng and Xu "Return to Adaptation in a Changing Climate".

Table O.1: Cyclone sample moments for each country

| ISO Code | Country Name | M1 | Var | M3 | M4 | AC |
|---|---|---|---|---|---|---|
| AUS | Australia | 0.976 | 0.024 | -0.023 | 0.022 | 0.975 |
| BGD | Bangladesh | 0.195 | 0.157 | 0.096 | 0.083 | 0.050 |
| BHS | Bahamas, The | 0.098 | 0.088 | 0.071 | 0.065 | 0.025 |
| BLZ | Belize | 0.293 | 0.207 | 0.086 | 0.078 | 0.100 |
| BRA | Brazil | 0.049 | 0.046 | 0.042 | 0.040 | 0.000 |
| BRN | Brunei Darussalam | 0.220 | 0.171 | 0.096 | 0.083 | 0.075 |
| BWA | Botswana | 0.049 | 0.046 | 0.042 | 0.040 | 0.000 |
| CAN | Canada | 0.634 | 0.232 | -0.062 | 0.071 | 0.425 |
| CHN | China | 0.976 | 0.024 | -0.023 | 0.022 | 0.975 |
| COL | Colombia | 0.049 | 0.046 | 0.042 | 0.040 | 0.000 |
| CRI | Costa Rica | 0.293 | 0.207 | 0.086 | 0.078 | 0.100 |
| CUB | Cuba | 0.463 | 0.249 | 0.018 | 0.063 | 0.125 |
| DOM | Dominican Republic | 0.293 | 0.207 | 0.086 | 0.078 | 0.075 |
| ESP | Spain | 0.098 | 0.088 | 0.071 | 0.065 | 0.000 |
| FJI | Fiji | 0.244 | 0.184 | 0.094 | 0.082 | 0.100 |
| FRA | France | 0.049 | 0.046 | 0.042 | 0.040 | 0.000 |
| GBR | United Kingdom | 0.073 | 0.068 | 0.058 | 0.054 | 0.000 |
| GIN | Guinea | 0.049 | 0.046 | 0.042 | 0.040 | 0.000 |
| GNB | Guinea-Bissau | 0.049 | 0.046 | 0.042 | 0.040 | 0.000 |
| GRL | Greenland | 0.049 | 0.046 | 0.042 | 0.040 | 0.000 |
| GTM | Guatemala | 0.220 | 0.171 | 0.096 | 0.083 | 0.075 |
| HND | Honduras | 0.220 | 0.171 | 0.096 | 0.083 | 0.075 |
| HTI | Haiti | 0.171 | 0.142 | 0.093 | 0.081 | 0.050 |
| IDN | Indonesia | 0.220 | 0.171 | 0.096 | 0.083 | 0.075 |
| IND | India | 0.805 | 0.157 | -0.096 | 0.083 | 0.375 |
| IRL | Ireland | 0.049 | 0.046 | 0.042 | 0.040 | 0.000 |
| IRN | Iran, Islamic Rep. | 0.049 | 0.046 | 0.042 | 0.040 | 0.000 |
| ISL | Iceland | 0.049 | 0.046 | 0.042 | 0.040 | 0.000 |
| JAM | Jamaica | 0.049 | 0.046 | 0.042 | 0.040 | 0.000 |
| JPN | Japan | 0.976 | 0.024 | -0.023 | 0.022 | 0.950 |
| KHM | Cambodia | 0.244 | 0.184 | 0.094 | 0.082 | 0.100 |
| KOR | Korea, Rep. | 0.707 | 0.207 | -0.086 | 0.078 | 0.450 |
| LAO | Lao PDR | 0.902 | 0.088 | -0.071 | 0.065 | 0.850 |
| LKA | Sri Lanka | 0.049 | 0.046 | 0.042 | 0.040 | 0.000 |

Cyclone sample moments for each country, continued

| ISO Code | Country Name | M1 | Var | M3 | M4 | AC |
|---|---|---|---|---|---|---|
| MDG | Madagascar | 0.829 | 0.142 | -0.093 | 0.081 | 0.675 |
| MEX | Mexico | 0.976 | 0.024 | -0.023 | 0.022 | 0.950 |
| MNG | Mongolia | 0.049 | 0.046 | 0.042 | 0.040 | 0.000 |
| MOZ | Mozambique | 0.561 | 0.246 | -0.030 | 0.064 | 0.325 |
| MUS | Mauritius | 0.049 | 0.046 | 0.042 | 0.040 | 0.000 |
| MWI | Malawi | 0.049 | 0.046 | 0.042 | 0.040 | 0.000 |
| MYS | Malaysia | 0.220 | 0.171 | 0.096 | 0.083 | 0.075 |
| NAM | Namibia | 0.049 | 0.046 | 0.042 | 0.040 | 0.000 |
| NGA | Nigeria | 0.049 | 0.046 | 0.042 | 0.040 | 0.000 |
| NIC | Nicaragua | 0.317 | 0.217 | 0.079 | 0.076 | 0.100 |
| NOR | Norway | 0.049 | 0.046 | 0.042 | 0.040 | 0.000 |
| NZL | New Zealand | 0.122 | 0.107 | 0.081 | 0.073 | 0.050 |
| OMN | Oman | 0.049 | 0.046 | 0.042 | 0.040 | 0.000 |
| PAK | Pakistan | 0.098 | 0.088 | 0.071 | 0.065 | 0.000 |
| PAN | Panama | 0.293 | 0.207 | 0.086 | 0.078 | 0.100 |
| PHL | Philippines | 0.951 | 0.046 | -0.042 | 0.040 | 0.900 |
| PNG | Papua New Guinea | 0.049 | 0.046 | 0.042 | 0.040 | 0.000 |
| PRI | Puerto Rico | 0.122 | 0.107 | 0.081 | 0.073 | 0.050 |
| PRT | Portugal | 0.049 | 0.046 | 0.042 | 0.040 | 0.000 |
| RUS | Russian Federation | 0.610 | 0.238 | -0.052 | 0.068 | 0.350 |
| SEN | Senegal | 0.073 | 0.068 | 0.058 | 0.054 | 0.025 |
| SLB | Solomon Islands | 0.073 | 0.068 | 0.058 | 0.054 | 0.025 |
| SLV | El Salvador | 0.293 | 0.207 | 0.086 | 0.078 | 0.100 |
| SWZ | Eswatini | 0.049 | 0.046 | 0.042 | 0.040 | 0.000 |
| THA | Thailand | 0.780 | 0.171 | -0.096 | 0.083 | 0.625 |
| TTO | Trinidad and Tobago | 0.049 | 0.046 | 0.042 | 0.040 | 0.000 |
| SGP | Singapore | 0.220 | 0.171 | 0.096 | 0.083 | 0.075 |
| TZA | Tanzania | 0.561 | 0.246 | -0.030 | 0.064 | 0.600 |
| USA | United States | 0.976 | 0.024 | -0.023 | 0.022 | 0.975 |
| VEN | Venezuela, RB | 0.073 | 0.068 | 0.058 | 0.054 | 0.025 |
| VNM | Vietnam | 0.976 | 0.024 | -0.023 | 0.022 | 0.950 |
| VUT | Vanuatu | 0.122 | 0.107 | 0.081 | 0.073 | 0.025 |
| YEM | Yemen, Rep. | 0.049 | 0.046 | 0.042 | 0.040 | 0.000 |
| ZAF | South Africa | 0.049 | 0.046 | 0.042 | 0.040 | 0.000 |
| ZWE | Zimbabwe | 0.122 | 0.107 | 0.081 | 0.073 | 0.025 |

Table O.2: Heatwave sample moments for each country

| ISO Code | Country Name | M1 | Var | M3 | M4 | AC |
|---|---|---|---|---|---|---|
| AGO | Angola | 0.200 | 0.160 | 0.096 | 0.083 | 0.154 |
| ALB | Albania | 0.425 | 0.244 | 0.037 | 0.065 | 0.308 |
| ARE | United Arab Emirates | 0.150 | 0.128 | 0.089 | 0.079 | 0.103 |
| AUS | Australia | 0.225 | 0.174 | 0.096 | 0.083 | 0.205 |
| AUT | Austria | 0.200 | 0.160 | 0.096 | 0.083 | 0.051 |
| BDI | Burundi | 0.425 | 0.244 | 0.037 | 0.065 | 0.308 |
| BEL | Belgium | 0.325 | 0.219 | 0.077 | 0.075 | 0.154 |
| BEN | Benin | 0.050 | 0.048 | 0.043 | 0.041 | 0.000 |
| BFA | Burkina Faso | 0.350 | 0.228 | 0.068 | 0.072 | 0.256 |
| BGR | Bulgaria | 0.300 | 0.210 | 0.084 | 0.078 | 0.205 |
| BHS | Bahamas, The | 0.350 | 0.228 | 0.068 | 0.072 | 0.205 |
| BOL | Bolivia | 0.250 | 0.188 | 0.094 | 0.082 | 0.205 |
| BRA | Brazil | 0.300 | 0.210 | 0.084 | 0.078 | 0.231 |
| BWA | Botswana | 0.375 | 0.234 | 0.059 | 0.070 | 0.154 |
| CAF | Central African Republic | 0.175 | 0.144 | 0.094 | 0.082 | 0.154 |
| CAN | Canada | 0.200 | 0.160 | 0.096 | 0.083 | 0.051 |
| CHE | Switzerland | 0.100 | 0.090 | 0.072 | 0.066 | 0.026 |
| CHL | Chile | 0.025 | 0.024 | 0.023 | 0.023 | 0.000 |
| CHN | China | 0.050 | 0.048 | 0.043 | 0.041 | 0.000 |
| CIV | Cote d'Ivoire | 0.150 | 0.128 | 0.089 | 0.079 | 0.077 |
| CMR | Cameroon | 0.275 | 0.199 | 0.090 | 0.080 | 0.256 |
| COD | Congo, Dem. Rep. | 0.175 | 0.144 | 0.094 | 0.082 | 0.103 |
| COG | Congo, Rep. | 0.050 | 0.048 | 0.043 | 0.041 | 0.000 |
| COL | Colombia | 0.225 | 0.174 | 0.096 | 0.083 | 0.205 |
| CPV | Cabo Verde | 0.225 | 0.174 | 0.096 | 0.083 | 0.154 |
| CRI | Costa Rica | 0.600 | 0.240 | -0.048 | 0.067 | 0.436 |
| CUB | Cuba | 0.025 | 0.024 | 0.023 | 0.023 | 0.000 |
| CYP | Cyprus | 0.075 | 0.069 | 0.059 | 0.055 | 0.000 |
| DEU | Germany | 0.275 | 0.199 | 0.090 | 0.080 | 0.128 |
| DNK | Denmark | 0.250 | 0.188 | 0.094 | 0.082 | 0.128 |
| DOM | Dominican Republic | 0.100 | 0.090 | 0.072 | 0.066 | 0.051 |
| DZA | Algeria | 0.525 | 0.249 | -0.012 | 0.063 | 0.385 |
| ECU | Ecuador | 0.250 | 0.188 | 0.094 | 0.082 | 0.205 |
| EGY | Egypt, Arab Rep. | 0.300 | 0.210 | 0.084 | 0.078 | 0.282 |
| ESP | Spain | 0.400 | 0.240 | 0.048 | 0.067 | 0.231 |
| ETH | Ethiopia | 0.275 | 0.199 | 0.090 | 0.080 | 0.205 |
| FIN | Finland | 0.450 | 0.248 | 0.025 | 0.064 | 0.308 |
| FJI | Fiji | 0.225 | 0.174 | 0.096 | 0.083 | 0.205 |
| FRA | France | 0.250 | 0.188 | 0.094 | 0.082 | 0.103 |
| GAB | Gabon | 0.125 | 0.109 | 0.082 | 0.073 | 0.103 |
| GBR | United Kingdom | 0.050 | 0.048 | 0.043 | 0.041 | 0.000 |
| GEO | Georgia | 0.250 | 0.188 | 0.094 | 0.082 | 0.154 |
| GHA | Ghana | 0.200 | 0.160 | 0.096 | 0.083 | 0.154 |
| GIN | Guinea | 0.275 | 0.199 | 0.090 | 0.080 | 0.231 |
| GMB | Gambia, The | 0.225 | 0.174 | 0.096 | 0.083 | 0.205 |
| GNB | Guinea-Bissau | 0.100 | 0.090 | 0.072 | 0.066 | 0.026 |
| GNQ | Equatorial Guinea | 0.325 | 0.219 | 0.077 | 0.075 | 0.282 |
| GRC | Greece | 0.125 | 0.109 | 0.082 | 0.073 | 0.051 |
| GTM | Guatemala | 0.900 | 0.090 | -0.072 | 0.066 | 0.872 |
| HND | Honduras | 0.500 | 0.250 | 0.000 | 0.063 | 0.359 |
| HUN | Hungary | 0.275 | 0.199 | 0.090 | 0.080 | 0.103 |
| IRL | Ireland | 0.075 | 0.069 | 0.059 | 0.055 | 0.026 |
| IRN | Iran, Islamic Rep. | 0.350 | 0.228 | 0.068 | 0.072 | 0.256 |
| IRQ | Iraq | 0.375 | 0.234 | 0.059 | 0.070 | 0.256 |
| ISL | Iceland | 0.200 | 0.160 | 0.096 | 0.083 | 0.077 |
| ISR | Israel | 0.075 | 0.069 | 0.059 | 0.055 | 0.051 |
| ITA | Italy | 0.250 | 0.188 | 0.094 | 0.082 | 0.154 |
| JAM | Jamaica | 0.050 | 0.048 | 0.043 | 0.041 | 0.000 |
| JOR | Jordan | 0.250 | 0.188 | 0.094 | 0.082 | 0.231 |
| JPN | Japan | 0.075 | 0.069 | 0.059 | 0.055 | 0.026 |
| KEN | Kenya | 0.300 | 0.210 | 0.084 | 0.078 | 0.205 |
| KHM | Cambodia | 0.075 | 0.069 | 0.059 | 0.055 | 0.026 |
| KOR | Korea, Rep. | 0.050 | 0.048 | 0.043 | 0.041 | 0.000 |
| KWT | Kuwait | 0.475 | 0.249 | 0.012 | 0.063 | 0.333 |

Heatwave sample moments for each country, continued

| ISO Code | Country Name | M1 | Var | M3 | M4 | AC |
|---|---|---|---|---|---|---|
| LAO | Lao PDR | 0.225 | 0.174 | 0.096 | 0.083 | 0.128 |
| LBN | Lebanon | 0.600 | 0.240 | -0.048 | 0.067 | 0.538 |
| LKA | Sri Lanka | 0.150 | 0.128 | 0.089 | 0.079 | 0.077 |
| LSO | Lesotho | 0.225 | 0.174 | 0.096 | 0.083 | 0.205 |
| LUX | Luxembourg | 0.150 | 0.128 | 0.089 | 0.079 | 0.051 |
| LVA | Latvia | 0.575 | 0.244 | -0.037 | 0.065 | 0.385 |
| MAR | Morocco | 0.375 | 0.234 | 0.059 | 0.070 | 0.256 |
| MDG | Madagascar | 0.250 | 0.188 | 0.094 | 0.082 | 0.231 |
| MEX | Mexico | 0.225 | 0.174 | 0.096 | 0.083 | 0.205 |
| MLI | Mali | 0.275 | 0.199 | 0.090 | 0.080 | 0.128 |
| MNG | Mongolia | 0.475 | 0.249 | 0.012 | 0.063 | 0.333 |
| MOZ | Mozambique | 0.100 | 0.090 | 0.072 | 0.066 | 0.026 |
| MRT | Mauritania | 0.100 | 0.090 | 0.072 | 0.066 | 0.026 |
| MUS | Mauritius | 0.125 | 0.109 | 0.082 | 0.073 | 0.077 |
| MWI | Malawi | 0.450 | 0.248 | 0.025 | 0.064 | 0.333 |
| MYS | Malaysia | 0.025 | 0.024 | 0.023 | 0.023 | 0.000 |
| NAM | Namibia | 0.450 | 0.248 | 0.025 | 0.064 | 0.256 |
| NER | Niger | 0.125 | 0.109 | 0.082 | 0.073 | 0.077 |
| NGA | Nigeria | 0.075 | 0.069 | 0.059 | 0.055 | 0.026 |
| NIC | Nicaragua | 0.525 | 0.249 | -0.012 | 0.063 | 0.385 |
| NLD | Netherlands | 0.375 | 0.234 | 0.059 | 0.070 | 0.179 |
| NOR | Norway | 0.325 | 0.219 | 0.077 | 0.075 | 0.205 |
| NPL | Nepal | 0.100 | 0.090 | 0.072 | 0.066 | 0.051 |
| NZL | New Zealand | 0.025 | 0.024 | 0.023 | 0.023 | 0.000 |
| OMN | Oman | 0.225 | 0.174 | 0.096 | 0.083 | 0.205 |
| PAK | Pakistan | 0.075 | 0.069 | 0.059 | 0.055 | 0.026 |
| PAN | Panama | 0.150 | 0.128 | 0.089 | 0.079 | 0.051 |
| PER | Peru | 0.300 | 0.210 | 0.084 | 0.078 | 0.231 |
| PNG | Papua New Guinea | 0.225 | 0.174 | 0.096 | 0.083 | 0.205 |
| POL | Poland | 0.300 | 0.210 | 0.084 | 0.078 | 0.128 |
| PRT | Portugal | 0.125 | 0.109 | 0.082 | 0.073 | 0.051 |
| PRY | Paraguay | 0.250 | 0.188 | 0.094 | 0.082 | 0.205 |
| QAT | Qatar | 0.400 | 0.240 | 0.048 | 0.067 | 0.282 |
| RWA | Rwanda | 0.350 | 0.228 | 0.068 | 0.072 | 0.205 |
| SAU | Saudi Arabia | 0.175 | 0.144 | 0.094 | 0.082 | 0.103 |
| SDN | Sudan | 0.175 | 0.144 | 0.094 | 0.082 | 0.128 |
| SEN | Senegal | 0.325 | 0.219 | 0.077 | 0.075 | 0.231 |
| SLE | Sierra Leone | 0.050 | 0.048 | 0.043 | 0.041 | 0.000 |
| SLV | El Salvador | 0.625 | 0.234 | -0.059 | 0.070 | 0.513 |
| SWE | Sweden | 0.175 | 0.144 | 0.094 | 0.082 | 0.077 |
| SWZ | Eswatini | 0.225 | 0.174 | 0.096 | 0.083 | 0.103 |
| SYR | Syrian Arab Republic | 0.325 | 0.219 | 0.077 | 0.075 | 0.205 |
| TCD | Chad | 0.225 | 0.174 | 0.096 | 0.083 | 0.128 |
| TGO | Togo | 0.275 | 0.199 | 0.090 | 0.080 | 0.231 |
| THA | Thailand | 0.025 | 0.024 | 0.023 | 0.023 | 0.000 |
| TTO | Trinidad and Tobago | 0.300 | 0.210 | 0.084 | 0.078 | 0.231 |
| TUN | Tunisia | 0.550 | 0.248 | -0.025 | 0.064 | 0.462 |
| TUR | Turkey | 0.250 | 0.188 | 0.094 | 0.082 | 0.179 |
| TZA | Tanzania | 0.025 | 0.024 | 0.023 | 0.023 | 0.000 |
| UGA | Uganda | 0.300 | 0.210 | 0.084 | 0.078 | 0.205 |
| URY | Uruguay | 0.050 | 0.048 | 0.043 | 0.041 | 0.000 |
| USA | United States | 0.125 | 0.109 | 0.082 | 0.073 | 0.051 |
| VEN | Venezuela, RB | 0.225 | 0.174 | 0.096 | 0.083 | 0.128 |
| VUT | Vanuatu | 0.250 | 0.188 | 0.094 | 0.082 | 0.231 |
| ZAF | South Africa | 0.200 | 0.160 | 0.096 | 0.083 | 0.179 |
| ZMB | Zambia | 0.475 | 0.249 | 0.012 | 0.063 | 0.282 |
| ZWE | Zimbabwe | 0.300 | 0.210 | 0.084 | 0.078 | 0.205 |

Table O.3: Summary statistics of sample moments across all countries

This table shows the summary statistics of country-level cyclone and heatwave sample moments across all countries. M1 is the mean of arrivals, Var is the variance, M3 is the 3rd central moment, M4 is the 4th central moment, and AC is the first-order autocorrelation, defined as the sample analogue of $\mathbb{E}[D_t D_{t-1}]$.

| Panel A: Cyclone sample moments | | | | | |
|---|---|---|---|---|---|
| | Mean | S.D. | Median | P10 | P90 |
| M1 | 0.29 | 0.32 | 0.12 | 0.05 | 0.95 |
| Var | 0.10 | 0.07 | 0.07 | 0.05 | 0.21 |
| M3 | 0.04 | 0.05 | 0.04 | -0.04 | 0.09 |
| M4 | 0.06 | 0.02 | 0.05 | 0.04 | 0.08 |
| AC | 0.19 | 0.31 | 0.05 | 0.00 | 0.90 |
| **Panel B: Heatwave sample moments** | | | | | |
| | Mean | S.D. | Median | P10 | P90 |
| M1 | 0.25 | 0.16 | 0.23 | 0.05 | 0.45 |
| Var | 0.16 | 0.07 | 0.17 | 0.05 | 0.24 |
| M3 | 0.06 | 0.04 | 0.08 | 0.02 | 0.10 |
| M4 | 0.07 | 0.02 | 0.07 | 0.04 | 0.08 |
| AC | 0.17 | 0.14 | 0.15 | 0.00 | 0.31 |

Table O.4: Panel regression estimates of the risk-dependent model

This table shows the estimation results of our risk-dependent model in a pooled panel regression. $t$-statistics (with bootstrapped standard errors) are shown in parentheses. ***, **, and * denote statistical significance at the 1%, 5%, and 10% levels respectively.

| | Cyclone | Heatwave |
|---|---|---|
| $\hat{\beta}_1$ | -0.992*** | -0.682*** |
| | (-15.0) | (-13.4) |
| $\hat{\beta}_2$ | 0.177** | 0.148*** |
| | (2.28) | (2.63) |
| Country FE | Yes | Yes |
| Year FE | Yes | Yes |

Figure O.1: Density of $\hat{\beta}_{1i}$ and $\hat{\beta}_{2i}$ after detrending

This figure plots the density (estimated using the Epanchnikov kernel) of the individual $\hat{\beta}_{1i}$ and $\hat{\beta}_{2i}$ estimated from the detrended version of our main equation (8).

Panel A: Density plot of $\hat{\beta}_{1i}$

Cyclone $\hat{\beta}_{1i}$

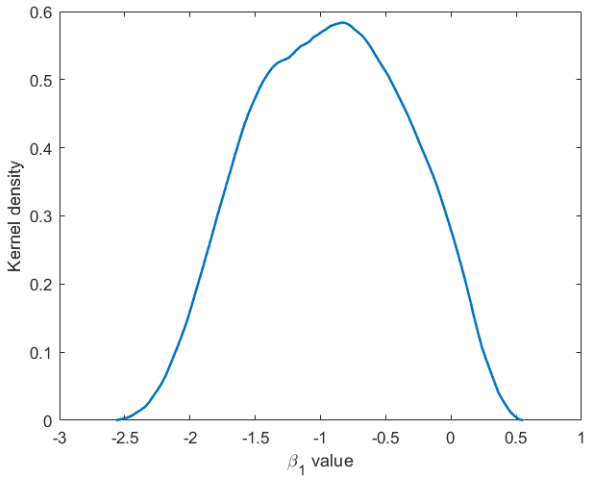


Heatwave $\hat{\beta}_{1i}$

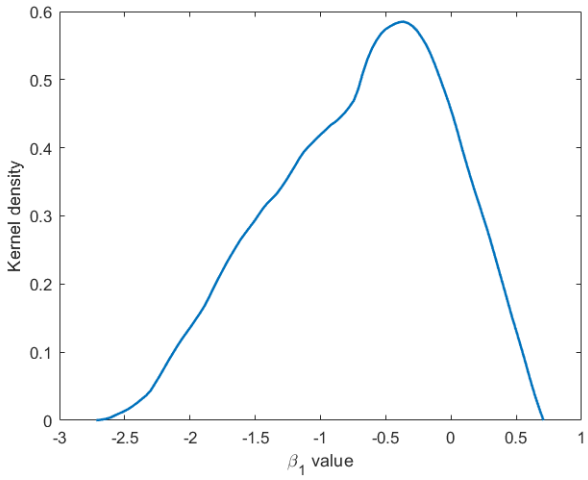


Panel B: Density plot of $\hat{\beta}_{2i}$

Cyclone $\hat{\beta}_{2i}$

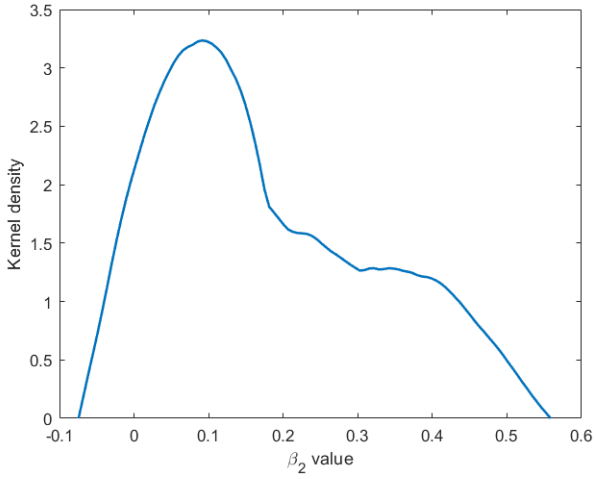


Heatwave $\hat{\beta}_{2i}$

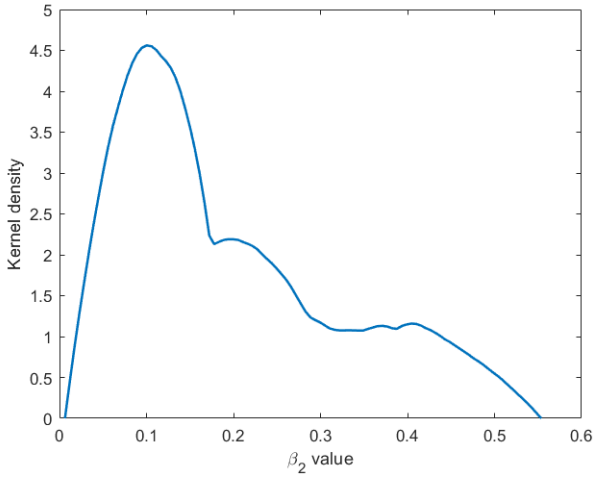

Table O.5: Summary statistics of projected real GDP per capita in 2050, mixture model, higher order Taylor approximation

This table presents the summary statistics of projected real GDP per capita across countries in 2050 using the mixture model simulation for both the cyclone and the heatwave sample. Real GDP per capita is in thousands of constant 2015 USD. Adaptation is our main adaptation function with the first-order Taylor approximation. Adaptation order 2 is the adaptation function with the second-order Taylor approximation.

| Projected real GDP per capita in 2050, higher order Taylor approximation | | | | |
|---|---|---|---|---|
| | Cyclone sample | | Heatwave sample | |
| | Adaptation | Adaptation order 2 | Adaptation | Adaptation order 2 |
| Mean | 31.8 | 32.1 | 30.9 | 31.3 |
| S.D. | 26.6 | 26.9 | 29.5 | 29.8 |
| Median | 21.2 | 21.4 | 17.9 | 18.1 |
| P5 | 6.3 | 6.3 | 4.8 | 4.9 |
| P25 | 13.9 | 14.0 | 10.2 | 10.4 |
| P75 | 40.7 | 41.0 | 41.4 | 41.6 |
| P95 | 82.3 | 83.9 | 86.8 | 88.4 |